UNIVERSITY OF THESSALY

POLYTECHNIC SCHOOL

DEPARTMENT OF MECHANICAL ENGINEERING

LABORATORY OF MATERIALS

Diploma Thesis

"Study of Intercritical Annealing of DP1000 Steel"

By

Georgios C. Nanas

Supervisor:

Dr. Helen Kamoutsi

Submitted for the Partial Fulfillment of the requirements for

the degree of Diploma in Mechanical Engineering

Certified by the members of the Thesis Committee:

First Examiner (Supervisor)

Dr. Helen Kamoutsi

Lab Teaching Staff

Department of Mechanical Engineering

University of Thessaly

Second Examiner

Dr. Nikolaos Aravas

Professor of Computational Mechanics of Structures

Department of Mechanical Engineering

University of Thessaly

Third Examiner

Dr. Alexis Kermanidis

Assistant Professor of Mechanical Behaviour of Metallic Materials

Department of Mechanical Engineering

University of Thessaly

Table of Contents

Table of Figures

Table of Tables

Acknowledgements

This project was accomplished in the scope of the partial fulfillment of the requirements for the degree of Diploma in Mechanical Engineering at University of Thessaly.

I would first like to express my sincere gratitude to my supervisor Dr. Helen Kamoutsi, whose expertise was invaluable in the formulating of the research topic and methodology in particular. The door to Dr. Kamoutsi's office was always open whenever I needed to communicate with her. It was her inexhaustible patience, her valuable input and guidance throughout both the experimental and theoretical part that led to the completion of my Diploma Thesis.

Further, I am particularly grateful to Professor Nikolaos Aravas and Assistant Professor Alexis Kermanidis for accepting to take part in the three member evaluation committee of my Diploma Thesis.

My special thanks are extended to all of my co-students and co-workers in the Laboratory of Materials for their constructive conversations, their advice and assistance during my entire engagement in the lab. Their support was, at times, more than precious. I would particularly like to single out Dr. Anna Zervaki for her patience throughout this period of time and her treating me as a member of the Laboratory.

I would also like to thank my friends, who were of great support in deliberating over our problems and findings, as well as providing happy distraction to ease my mind outside my research.

Last but not least, I would like to express my gratitude to my parents, Chrysostomos and Stella, for their uninterrupted support and wise counsel throughout the course of my studies, that made me confident and wiser and helped me face all the difficulties that have arisen, as well as my sister Katerina for her unconditional love and support and her being my most valuable advisor and avid supporter.

Abstract

A systematic experimental study has been conducted on intercritical austenite formation during intercritical annealing and subsequent martensite formation during quenching for a steel with chemical compositions typically used for dual-phase and transformation-induced plasticity (TRIP) steels. The steel grade was DP1000. Different initial heating temperatures, and holding times were applied to the material to examine the austenite and martensite formation kinetics. Image analysis techniques as well as thermodynamic calculations were employed. It was found that the initial microstructure of the specimen affects the isothermal austenite formation kinetics. This can be attributed to the interaction between austenite and martensite formation processes. Austenite is to a large extent randomly distributed in the ferrite matrix. Ferrite grains have varying grain sizes and martensite can be observed in the ferrite matrix both as equiaxed grains as well as plate martensite. Volume fraction of martensite after quenching was evaluated with thermodynamic calculations and image analysis techniques. The microharness of the specimen was measured, and it was found largely dependent on the intercritical annealing temperature.

Chapter 1: Introduction

Description of the problem

In recent years, the automotive industry following the development of material technology strives to fulfill the demands of fuel economy and safety by optimizing vehicle's weight and crash performance respectively. Dual Phase (DP) steels are ideally suited for these demands combining high strength and ductility. Their microstructure consists of a soft ferritic matrix containing islands of hard martensite as a secondary phase. Ferrite contributes to the steel's ductility and martensite to its high strength. Combining both phases and their advantages, an extra advantageous kind of steel is created. To generate the required microstructures, a processing route can be used, which involves cold rolling of ferrite/pearlite microstructures followed by intercritical annealing on a continuous annealing line. Although a general understanding of these materials has been developed, a number of fundamental issues remain to be solved. A careful control of processing conditions and the identification of critical processing steps is crucial to the success of these products. The challenge, therefore, is to develop industrially relevant processing routes that will lead to the desired properties with a minimum of variation. The processing routes for cold-rolled and annealed dual phase involve reheating the steel into the intercritical region, where an austenite/ferrite mixture is formed. For dual-phase steels, cooling to room temperature produces a microstructure consisting of ferrite and martensite. The cooling path and composition of these steels must be carefully optimized to minimize transformation back to ferrite or the pearlite and bainite reactions. This is usually facilitated by alloy additions such as Mn, Mo, or Cr and by employing the optimum heat treatment.

In the present work the formation of austenite during intercritical annealing at temperatures between 700^{o}C and 780^{o}C was studied for a DP1000 steel containing 0.07 carbon and 2.54 Mn and with a ferrite-pearlite starting microstructure, typical of most dual-phase steels. Austenite formation was separated into three stages: (1) very rapid growth of austenite into pearlite until pearlite dissolution is complete; (2) slower growth of austenite into ferrite at a rate that is controlled by carbon diffusion in austenite at high temperatures (760^{o}C) and by manganese diffusion in ferrite (or along grain boundaries) at low temperatures (3) very slow final equilibration of ferrite and austenite at a rate that is controlled by manganese diffusion in austenite.

Thesis objective

In view of the above considerations, the present thesis tries to answer the question posted above, i.e. what is the best process route to generate the required microstructures, in a dual-phase steels?

The thesis objectives are therefore the following:

1. To establish a link between the thermodynamic and kinetic calculations that were produced as a result of the RFCS project TOOLKIT and the experimental results performed in the current study.

2. To better understand the link between heat treatment and resulting microstructure and mechanical properties in DP steel 1000.

Thesis methodology

Research was focused on Cold Rolled (CR) Dual Phase (DP) steel with grade 700Y980T. The experimental procedures involved the following actions:

1) Heat treatments

2) Metallography (optical microscopy)

4) Image Analysis

5) Thermodynamic Calculations (Thermocalc -TCFE6)

6) Micro hardness tests

Thesis outline

The thesis outline is as follows

Chapter 1 - Introduction
Chapter 2 - Literature Review
Chapter 3 - Experimental Procedures
Chapter 4 - Results and Discussion
Chapter 5 - Conclusions
Chapter 6 – Proposed Future Work

Chapter 2: Bibliographic Review

In the modern era, automotive industry has to keep up with the contemporary demands of our society, which requires not only the weight reduction of transportation equipment, driving to fossil fuels savings and greenhouse gases limitations, but also the construction of safe vehicles [1]. Dual phase steels are ideal for these demands of modern automotive industry. Their microstructure consists of a soft ferritic matrix, that makes them ductile and a second martensitic phase which is embedded in pockets giving also high tensile strength (for DP1000 steels $\sigma_{UTS}\approx$1000 MPa). These advantages combined with low yield point (due to the absence of Lüders bands), good dynamic behavior, large tensile elongation, good cold formability and weldability make dual phase steels suitable for complex structural parts such as side members, cross members, stretch formed exterior parts and crash relevant components. Last but not least, one of the most important characteristics that make dual phase steels suitable for crash relevant parts is the high energy absorbing ability, which is related to the binary microstructure taking advantage of all beneficial characteristics of both phases [2]. The result is the construction of eco-friendly, safe, comfortable and low production and cost vehicles. All these contribute to weight optimization, safety and economy, three of the main goals of automotive industry [1-3].

Microstructure and properties in DP1000 steels are formed by the combination of alloy elements with mechanical and thermal treatments, as in all steel grades. The behavior of each element depends and is modified by the presence of another element. The interaction of alloy elements and their combining action is a complex theme and affects both the thermodynamics and kinetics of phase transformation. For this reason, a sort description of the effects for every alloying element is presented below.

Carbon (C): Constitutes the most important element in steels contributing to their' strength. Increasing the weight percent in C, results in subsequent increase in hardness, durability and hardenability. While, ductility, toughness and weldability decrease.

Manganese (Mn): Contributes to the desulphurization of steel by creating sulfides (MnS) and improves workability and weldability. Moreover, adding Mn, the hardenability of steels increases.

Silicion (Si): Constitutes one of the two elements (the other one is Aluminum-Al) that are used for deoxidation of steels. Simultaneously, it promotes ferrite transformation.

Chromium (Cr): Cr is a strong carbidogen. Increase in carbide content, increases the steel hardness and its antifriction properties. Cr also increases hardenability and the resistance for oxidation and corrosion. It is also used in order to retard the formation of pearlite or bainite.

Molybdenum (Mo): A strong carbidogen element as well, that increases steel hardenability. Molybdenum carbides form during tempering after quenching. Mo is also used to prevent the pearlite or bainite formation.

Tungsten (W), Vanadium (V), Titanium (Ti), Niobium (Nb): These elements are carbidogen and result in the increase of hardness and durability with carbide formation, while they restrict grain growth at high temperatures. V and Nb are also used for precipitation hardening and for grain size refinement.

Cobalt (Co): Co is the only element that decreases hardenability, it does not form carbides and has little effect on the hardness of steel. Its main action is to impede grain growth during annealing or tempering of steel. In that way Co contributes to the conservation of mechanical resistance [4-6].

DP steels are an advantageous type of steel combining strength and ductility. Apart from the morphology, that demands homogeneously dispersed fine martensite particles and fine ferrite grains with an ultra-fine prior austenite grain size, factors like size, shape and distribution of the structural constituents play a vital role to the mechanical properties of DP steels. For that reason, initial microstructure and the route that the final two-phase (ferrite-martensite) microstructure is generated have a great influence on the mechanical properties [7].

Dual phase steels exhibit several different microstructures that mainly depend on the undergone heat treatment after either hot rolling or cold rolling. The ferrite/austenite percentage can change via heat treatments and this allows a great variation in microstructure to be produced, so that a wide range of mechanical properties can be obtained [8].

To generate a dual phase microstructure the steps that are followed include cold rolling (or hot rolling) of the material and subsequently intercritical annealing on a continuous annealing line. In the second step, usually, in the region between A_1 and A_3 temperatures, the existing microstructure is composed of ferrite and austenite. During this step heating rate is of greatest importance as it can lead to microstructures in a wide variety, from fully to partially recrystallized, before the formation of austenite [5]. The sequelae step of intercritical annealing is cooling of the steel to room temperature. This step must be carefully done because martensitic transformation requires rapid rates of cooling. Otherwise, transformation can drive to pearlite or bainite formation. According to Speich et. al. austenite formation can be separated into three stages: a) very rapid growth of austenite into pearlite until complete pearlite dissolution, b) slower growth of austenite into ferrite primarily controlled by carbon diffusion in austenite, c) very slow equilibration of austenite and ferrite controlled by Mn diffusion in austenite [9]. Favorable sites for austenite nucleation, as referred above, are ferrite-pearlite interfaces and cementite particles at ferrite grain boundaries [10, 11].

On occasion the annealing step is performed on high temperature austenite state above A_3 temperature, where the most of undercooled austenite forms ferrite and the rest amount is transformed into martensite, or on two-phase ferrite-austenite state between A_1 and A_3 temperatures [5, 12].

Great influence in the mechanical properties of a steel derives from the alloying elements, as they influence phase transformation providing an even greater control over microstructure [8]. Dual phase microstructures in proeutectoid steels can generally be obtained through intercritical annealing (IA) at a ferrite-austenite (two-phase) temperature, followed by quenching, during which austenite transforms to martensite [1]. Austenite usually cannot be found in final products and appears as an intermediate phase, which transforms either to pearlite or to martensite, depending on the cooling rate [11]. Final microstructure of a dual phase steel depends on the formation of austenite during intercritical annealing (IA), which is a diffusion controlled phase transformation combining nucleation and growth processes [13]. Nucleation is a process that gets started by the formation of little particles, called nuclei and lean to the formation of a new phase. Usually, nucleation is an heterogeneous process i.e. the nuclei formation is powered by imperfections of

structure like cavities, dislocations, grain boundaries or other interfaces. Growth is a process that follows nucleation of a new phase until this new phase reach an equilibrium percentage as it is defined from the phase diagram [4].

The starting microstructure of steel affects strongly the kinetics of austenitization. An initial microstructure that consists of ferrite and pearlite leads to a two-stage austenitization. The first step is the fast dissolution of pearlite, where nucleation of austenite occurs in ferrite/cementite boundaries and austenite grows rapidly in the pearlitic regions. This process is a fast one taking place between a few seconds and a few minutes. The second step is the formation of austenite from the initial ferrite. This is a slower process than the previous one and takes place under certain conditions, such as fast heating. Austenite forms on ferrite grain boundaries. The rate of its growth is affected by carbon diffusion in austenite. Austenite growth depends on the alloying elements and how they affect the A_3 (Ac_3) temperature. For instance, Manganese (Mn), which is austenite stabilizer drops the Ac_3 temperature and completes faster the austenite formation. On the other hand, elements, such as Silicon (Si), which are ferrite stabilizers, cause an increase in Ac_3 temperature and delay the formation of austenite [13].

During IA treatment, the dominant mechanisms in dual phase steels are recovery, recrystallization and phase transformation. According to Peranio et al. [14, 15] there is a complicated interaction between these metallurgical mechanisms, which are affected by heating rate, annealing temperature and time and cooling rate. According to Huang et al., recovery appears to be a negligible softening process in materials such as dual phase steels [10], and according to Matsumura et al. at intercritical annealing temperatures there are some sub-boundaries in the ferritic region that are formed by the recovery process of lath boundaries of original martensite during holding at intercritical annealing temperatures [7]. Therefore, during IA the two prevalent phenomena that are taking place are: recrystallization of ferrite and formation of austenite. It seems that these two phenomena are competing each other when heat treatment is above Ac_1 temperature, as ferrite recrystallization appears with retardation when austenite fraction (due to austenite formation) is above 30%. Peranio et al. [14, 15] pointed the interaction between recrystallization and phase transformation. They divided the intercritical annealing regime in three sub-regions. For low intercritical annealing temperatures they noticed full recrystallization within the first few seconds and thereafter, with a little time gap between, they noticed that hardness was continuously increased with annealing time, which indicates an ongoing phase transformation and thereby an increase of the volume fraction of martensite after quenching. For intermediate annealing temperature, the behavior of hardness with annealing time is similar to the case of low IA temperatures. However, phase transformation starts immediately after the end of recrystallization. Finally, for high IA temperatures, they noticed that minimum hardness of steel was higher than in cases with lower IA temperatures and that recrystallization was not complete when phase transformation started. All these lean towards the following conclusion: incubation time for phase transformation decreased with increasing annealing temperature and yielded a strong overlap of recrystallization and phase transformation for IA temperatures larger than the intermediate values in a range between 710^{o} and 830^{o} C. According to Ogawa [16] the fraction of non-recrystallized ferrite (F_{NR}) is a function of the fraction of recrystallized ferrite (F_R) and formatted austenite (F_γ): $F_{NR} = 100 - (F_R + F_\gamma)$. Increasing temperature, fractions of recrystallized ferrite and formatted austenite are increasing while fraction of non-recrystallized ferrite is decreasing. Austenite is formed mainly either at the recrystallized and non-recrystallized ferrite interface or at the grain boundaries of

recrystallized ferrite. The amount of formed austenite is increased as the temperature increases, but the more austenite formed the lower its carbon content will be and consequently its hardenability [17]. However, the growth of austenitic grains during intercritical annealing (IA) is impeded by the rapid heating rate. A conclusion that can be made is that in a rapid heating rate ferrite recrystallizes partially while there is full recrystallization of ferrite for low heating rates [11]. Austenite can be also generated in cementite particles or pearlite colonies. The pearlite or cementite dissolution, which occurs very rapidly, drives to the diffusion of carbon in the grain boundaries in order to, form austenite. Annealing for times longer than those required for complete pearlite dissolution resulted in a further increase in the volume fraction of austenite [9, 16, 18]

In cold rolled (CR) DP sheets, it seems that two main phenomena are taking place, as referred above. These are the recrystallization of deformed ferrite grains and the spheroidization of cementite particles. Concerning the transformation from pearlite to austenite in hot rolled (HR) DP steels, it is about a fast phase transformation that takes place between a few seconds and a few minutes. The main sites for austenite nucleation are mostly ferrite-pearlite interfaces and secondly the interface between pearlite colonies. For low heating rates, it seems that nucleation of austenite takes place at ferrite grain boundaries at the same time with the cases described above. In CR DP steels growth of austenite takes place at ferrite grain boundaries. Furthermore, according to Azizi-Alizamini, undissolved carbide particles are mostly spheroidized inside the ferritic matrix. At the temperature of the experiment of Azizi-Alizamini, the fraction of the transformed austenite is equal to the initial fraction of pearlite [11].

Concerning ferrite to austenite transformation, it is a diffusional mechanism. Austenite growth occurs not only by the transformation of the initial pearlite but austenite grows also into proeutectoid ferrite grains. It seems that there is a correlation between the heating rate and the different sites where nucleation occurs. According to Huang et al. [19] low heating rates lead to austenite growth at pearlitic sites while faster heating rates drive to nucleation at ferrite grain boundaries. This concerns only the hot rolled steels. More specifically, for hot rolled DP steels and low heating rates, islands of austenite seem to substitute entirely the pearlitic colonies of the as received metal. Grain boundaries and austenite remain distinct. Concerning high heating rates, austenite nucleates at ferrite grain boundaries in a way that a network of united austenite grains is created. It is like some chain links. For cold rolled dual phase (CR DP) steels, pearlite colonies take their final shape after cold rolling. Moreover, austenite nucleation occurs in the same time with recrystallization. For low heating rates, it was observed from metallographic analysis that ferrite recrystallization precedes that of austenite nucleation. On the other hand, for high heating rates austenitic islands are shaped. These islands are elongated and wider than the already elongated initial pearlite colonies. Another fact that is worth to be noticed is that there is no austenite formed in ferrite grain boundaries, but only very few particles of austenite. The fast rate of growth is capable of erasing the driving force required for nucleation at ferritic grain boundaries. The result is long and thick stripes of austenite parallel to the rolling direction [10].

Martensite is a hard phase that plays a key role in DP steels. Martensitic transformation happens when steel is heated above A_3 temperature, in the austenite field, or in the two-phase (ferrite-austenite) regime between A_1 and A_3 temperatures, followed by rapid cooling, usually water quenching or air cooling or oil quenching in other occasions. The deformation causes a change in the shape of the initial FCC austenite to the final transformed BCT martensite, which comes from the

shear transformation of the initial austenitic phase. Martensitic transformation is a non-diffusive and athermal one as martensite is formed by a deformation of austenite lattice without any diffusion of atoms. It has a high technological importance constituting the basis in technology and evolution of steels in a wide range. So, it is important to control the transformation, as in that way we can control the mechanical properties of the final product. A key role to the mechanical behavior plays the microstructure and its factors such as volume fraction of the existing phases, shape, size, spatial distribution and carbon content of the hard phase i.e. martensite.

Martensitic transformation is used for the increase of both hardness and durability. Its non-diffusive character is justified by the fact that rapid cooling rates are demanded in order to prevent and avoid other competitive diffusional transformations such as pearlitic or bainitic. According to Azizi-Alizamini, the cooling rate was approximately 1000K/s to ensure a complete austenite to martensite transformation after quenching. Furthermore, atomic diffusion is not required for the nucleation and growth of the martensitic phase [4, 11, 12].

The athermal character of the transformation means that martensite volume fraction does not increase with time, as very rapid nucleation and growth are taking place (times of the order of 10^{-7}s), but increases with temperature decrease between two characteristic temperatures, M_s and M_f, which indicate the start and the finish of the martensitic transformation respectively. Martensitic transformation starts when temperature drops below M_s, which has a strong dependence from steel's chemical composition. Alloying elements such as C, N, Ni, Mn, which are called austenite-stabilizers, drop M_s temperature because higher chemical driving force for martensite nucleation is required. Furthermore, other alloying elements that are not austenite-stabilizers, such as Cr, Mo, Al, Si, W, V can drop the M_s temperature, due to the fact that they cause solid solution strengthening in austenite and that results to the impeding of dislocation slip in order to form a martensitic nuclei. There are several empirical equations that calculate M_s temperature. One of them, maybe the most famous is Andrews's equation [20], that correlates M_s temperature with the percentage of each alloying element referred above:

$$M_s\ (^{o}C) = 539 - 423C - 30.4Mn - 17.7Ni - 12.1Cr - 7.5\ Mo \quad (1)$$

As it seems, carbon has the biggest contribution to Andrews equation. Another conclusion is that M_s temperature decreases with increasing carbon content.

One important parameter is intercritical annealing temperature. An increase on it contributes to the increase of martensite volume fraction. Simultaneously, that increase causes a change in the morphology of martensite. For low intercritical annealing temperatures, martensite is presented as a blocky type, while for higher one's martensite is shown in a lath type. The Mn content is responsible for the grain growth control during intercritical annealing [6]. In general, martensite has a lenticular shape with two main morphologies: plate martensite and lath martensite. For low carbon steels, like the examined DP1000 steel provided by ThyssenKrupp, martensite displays a lath type [4].

Austenite may not transform totally in martensite. In fact, there may be a little percentage of austenite than remains untransformed, which is called remained austenite. In fact, there is no martensite finish temperature M_f but for convenience, M_f is referred as the point that 95% of the martensitic transformation is completed [4, 8].

In DP1000 steels the goal is a microstructure that consists of 50% ferrite and 50% martensite, which has excellent mechanical properties in terms of tensile strength, ductility and fracture energy. A further increase in martensite volume fraction was found to decrease tensile strength and ductility [21]. In fact that DP1000 50-50 ratio is not actual, as a little percent, up to 7%, is retained austenite, which does not transform to martensite after quenching. This retained austenite fraction decreases with increasing annealing temperature and usually appears at the interface between austenite and ferrite during cooling. A reason of its presence may be the fact that martensite finish temperature (M_f) is depressed below room temperature, which is the final temperature after water quenching, so austenite cannot transform totally to martensite [17]. For an homogenous microstructure with well dispersed martensitic islands and fine recrystallized ferrite, a continuous annealing process is applied. The first step of this process is the reheat of a cold rolled ferrite-pearlite microstructure followed by intercritical annealing (IA). The result is a microstructure which consists of ferrite and austenite. The final step is water quenching resulting to the desirable microstructure of ferrite-martensite [9, 16, 18].

Concerning hardness, ferrite-martensite samples have higher hardness than the initial ferrite-pearlite ones. This higher hardness is known to be due to the presence of the hard martensitic phase. That 50% of martensite has also an important effect on the strength of the steel, especially on maximum ultimate strength. Nevertheless, one contradicting fact is that increasing the volume fraction of martensite, carbon content of the martensitic phase decreases. DP 1000 steels have another advantage that makes them suitable for vehicle parts and is the maximum value of total elongation that happens for a 50% of martensite. Further increase in martensite volume fraction beyond 50% changes the matrix structure from ferrite to martensite making the microstructure brittle [21]. Among the desired properties of DP steels are ductility and strength-toughness combination. Both are improved with the control of microstructure. Especially for the second, this combination is improved by microalloying elements such as V, Nb and Ti [6].

Speich et al. [22] studied the formation of austenite during intercritical annealing in three steels containing 1.5% Mn and 0.06, 0.12, and 0.20% carbon. The initial microstructure was fine-grained, unbanded ferrite-pearlite typical of most hot-rolled sheet steels used for production of dual-phase product. Combinationing dilatometric and quantitative metallographic techniques the volume fraction of austenite in these steels after intercritical annealing were evaluated. The kinetics of austenite formation were separated into three steps: 1) Nucleation of austenite at the ferrite-pearlite interface and very rapid growth of austenite into pearlite for very short times and low temperatures. At medium temperatures the times for dissolution of pearlite were much longer (15 s to 1 h). 2) After dissolution of pearlite, further growth of austenite into ferrite occurred. At high temperatures the growth of austenite was controlled by carbon diffusion in the austenite phase, and the times for completion of this step were short (2 to 9 s). At low temperatures the growth of austenite was controlled by manganese diffusion in the ferrite, and the times for completion of this step became much longer (4 to 24 h). 3) Final equilibration of the manganese contents of the austenite and ferrite phases was controlled by manganese diffusion in the austenite which is a much slower process than manganese diffusion in ferrite. The times for completion of this process were extraordinarily long (2000 to 4000 h).

Martensite can either deform plastically or not, depending on its carbon content. According to Bergstrom et al. for low carbon contents, martensite may start to deform plastically. Otherwise, for

high carbon contents, martensite remains elastic at least up to strains to necking [2]. Apart from martensite, plastic deformation in ferrite seems to start in ferrite grain boundaries i.e. in the neighborhood of martensitic particles. Deformation seems to be faster in the martensite sites than in regions beyond them. All these concerning deformation seems to be due to residual stresses remaining in the two phase interface after the austenite to martensite transformation firstly, and secondly due to the fact that during stress loading of the steel, large stresses will arise in the interface between ferrite-martensite, as martensite remains elastic till the value of the ultimate tensile stress (necking point)[2].

Iron and its alloys (steels) can be strengthened by several mechanisms such as work hardening, solid solution, dispersion strengthening and grain size refinement. The last one is of greatest importance in steels because provides one of the most important strengthening modes in the heat treatment of steels. Generally, grain size of polycrystalline materials is known to have great influence on their mechanical properties. It has reported that the smaller the grain size, the bigger the resulting yield ratio (i.e. the tensile to the ultimate tensile strength) [5]. Ferrite grain size seems to be very important affecting mechanical properties of dual phase steels, especially yield strength and secondly tensile strength. The influence of grain refinement to the strength of the steels is clearly presented by the Hall-Petch relationship between the yield stress σ_y and the grain diameter d :

$$\sigma_y = \sigma_0 + k_y d^{-1/2} \quad (2)$$

where σ_0 (friction stress) is constant and represents the yield stress of a single crystal and also the required stress to move dislocations along the slip planes in the BCC crystals. k_y, which is also constant, represents the slope of the $\sigma_y - d^{-1/2}$. Concerning martensitic transformation, the austenitic grain size determines the maximum size of martensitic plate. The conclusion coming from the Hall-Petch relationship is that the finer the grain size, the higher yield stress. For that reason nowadays, it is usual to produce steel sheets through rolling with grain sizes in the range 2-10 μm [8, 23]. According to Papa Rao et al., the usefulness of alloying elements such as V and Nb is to the grain size. For a DP steel intercritically annealed at 760^o C for 2 minutes with the presence of microportions of V and Nb, the ferrite grain size is 2μm, while with the absence of these two elements, grain size of ferrite for the same steel, for the same annealing procedure is 10μm [6].

Dual phase steels flow stress can be expressed as following: $\sigma = \sigma_A + \sigma_B$, where

σ_A : average stress in the soft ferritic phase.

σ_B : back stress, that is related to be the incompatibility of deformation between ferritic and martensitic phase [24].

In intercritical annealing the behavior of austenite formation is affected by prior austenite grain size. That's why heat treatment before intercritical annealing is so crucial. Fine ferrite grain size can also lead to high tensile strength, which is very important in dual phase steels. That increase via grain refinement is combined with the formation of sub-boundaries in ferritic zones during the recovery phenomenon [7].

Chapter 3: Experimental Procedures

1. Material Studied -

The material used for this project is a dual phase steel provided by ThyssenKrupp during the RFCS project TOOLKIT [25]. The steel grade is CR700Y980T-DP commonly known as DP 1000 steel and it was provided in metal sheet form. The chemical composition of the material is displayed below in Table 1.

Table 1: Chemical composition (%wt) of CR700Y980T-DP.

Materials	*Fe*	*C*	*Si*	*Mn*	*Cr*	*Mo*	*Cu*	*Al*	*Ti*	*V*	*Nb*	*W*	*Co*
DP1000	95.9758	0.07	0.298	2.5441	0.682	0.116	0.109	0.036	0.0719	0.0067	0.07	0.016	0.0045

The processing route for DP steels is depicted in Figure 1. The starting material is thin cold-rolled sheets with ferrite-pearlite or bainite microstructure Figure 2. The material is coiled after hot rolling at temperatures between 530-580°C. After pickling, the hot strip is cold rolled to a degree of 50-60% in order to achieve the targeted grain size after the following annealing stage (average grain size <2µm). The hot dip coated cold strip steel is then processed in a continuous annealing line. The heating rate is in the range between 50 to 70 °C/s. The annealing temperature is bounded between Ac_1 and Ac_3 and the desired amount of austenite during annealing is 50% γ. Typically, the temperatures are between 700°C and 850°C for times in the range of 50-100s.

Martensite is formed through the intercritical annealing (to obtain ferrite-austenite microstructure) and subsequent fast cooling. It is either quenched to room temperature or the quenching is interrupted to galvanize the sheet in hot dip galvanizing lines. The cooling rate in the upper temperature region has to exceed 10°C /s in order to avoid unwanted diffusional transformations. Due to the hot dip process, where the steel strip passes through a pot of liquid Zn, there is a stop of the cooling at about 460°C for about 20s [26, 27]. In Table 1.1 below the bounds for industrial thermal treatment of DP1000 steels are presented, which were provided by TKSE.

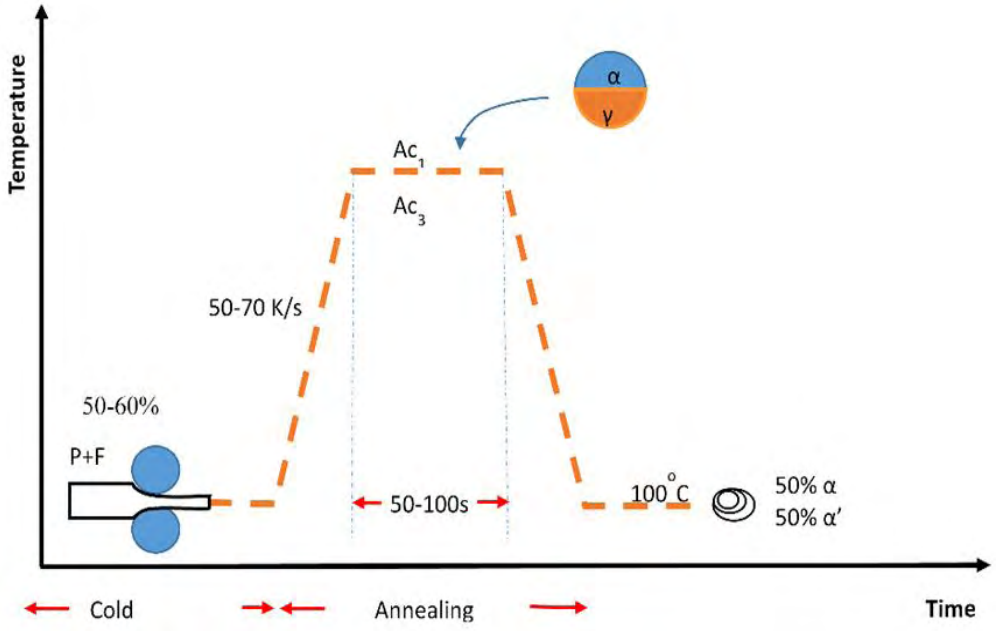

Figure 1: Schematic diagram of heat treatment of DP1000 steels.

Table 2: Bounds of industrial thermal treatment of DP1000 steels.

Process Parameters	Mean Values	Lower Bound	Upper Bound
Hot rolling Temperature [°C]	555	530	580
IA Temperature [°C]	775	700	850
IA Time [sec]	175	50	300
Finishing Temperature [°C]	100	100	100
Heating Rates [$°Cs^{-1}$]	60	50	70
Accelerated Cooling Rates [$°Cs^{-1}$]	55	10	100

The initial microstructure of the as received material is illustrated in Figure 2. It consists of 55% ferrite with grain size less than 2µm and 45% martensite with grain size less than 0.5µm.

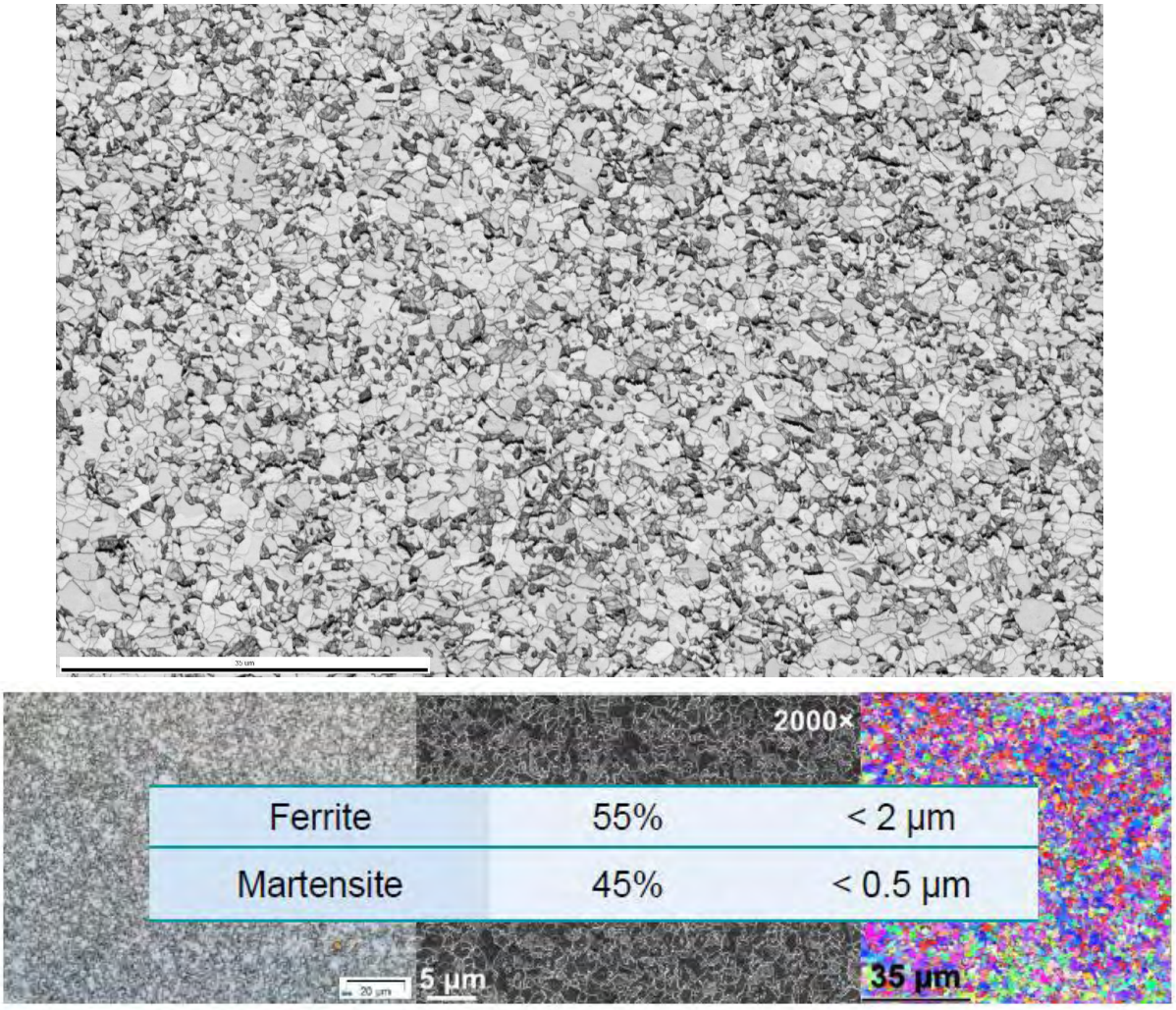

Figure 2: Initial microstructure of the as received material (DP1000) [25].

2. Specimen Preparation

Initially, the sheet material was cut in small specimens with a microtome (Struers Accutom) in the Laboratory of Materials (LoM). These specimens were rinsed with water and washed out with ethanol in order to, get rid of lubricants and impurities and to avoid corrosion. They were, then, dried under a warm air flow.

Schematically, a specimen used for the experiments is presented in the Figure 3. The dimensions were measured as follows: L = 15-18 mm, T = 10-12 mm and S =1.5 mm.

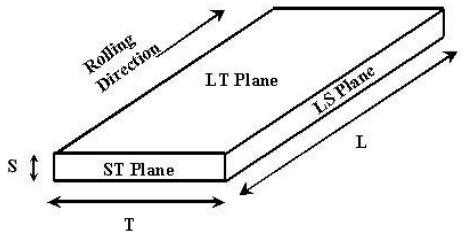

Figure 3: Labelling scheme used for directions and planes.

After the appropriated specimens were produced, they were subjected to the corresponding heat treatments.

3. Heat treatments

Heat treatments play a vital role in the processing of low alloy steels, such as DP1000. Heating rate is in industry an important factor that determines the final microstructure, due to the effect in the sites of nucleation during heating. In industrial level, long sheets or bulky masses of steel are used so that there is a point to diversify the rate of heating. In the present study, the material used is quite small. Therefore, high heating rates are applied, as the specimen being initially in room temperature reaches the desired temperature in a few seconds. Sometimes, when annealing times are small, a preheat method via warm air equal to a hair dryer is applied. It helps specimen to reach the already warmed furnace temperature quicker.

In the present study two heat treatments were applied. The initial heat treatment that was applied, prior to intercritical annealing, consists of heating in the full austenitic zone i.e. above 804^{o}C, more specifically at 854^{o}C, for 30 minutes and then isothermal holding at 550^{o}C, which the pearlitic region, for 60 minutes, this is illustrated in Table 3. Finally, all specimens were air cooled. This treatment had as a result a ferrite-pearlite microstructure, in accordance with the phase diagrams of DP 1000 steel. This initial step was performed in order to eliminate the original ultra fine grain size and create a new microstructure with larger and more distinct grains more easily observed with an optical microscope.

Another important parameter that concerns heat treatments is the annealing temperature. Intercritical annealing constitutes the second thermal treatment step. The intercritical temperature range for DP1000 lies between the Ae_1 and Ae_3 temperatures. The temperature at which austenite begins to form during heating (Ae_1) was calculated at 681.87^{o}C and the temperature at which the transformation of ferrite to austenite is completed during heating (Ae_3) was calculated at 803.42 ^{o}C, according thermodynamic calculations performed with ThermoCalc and the TCFE6 thermodynamic database. The temperatures that were implemented in the current work were 700 ^{o}C, 720 ^{o}C, 750^{o}C,

760°C, 770°C and 780°C, and intercritical annealing heat treatments were performed in order to compare the experimental results concerning volume fraction of the participating phases with results from simulations calculated during the RFCS project TOOLKIT [25]. Intercritical heat treatments of the specimens were performed in a vertical induction furnace for times ranging from 30 s to 1 h. The temperatures of IA and corresponding IA holding times along with specimen naming are presented in Table 4 to Table 6.
The final, but of greatest importance step is the cooling from the intercritical region to room temperature. This is achieved in all specimens via water quenching, immediately after IA in the laboratory furnace. This leads to martensite formation and generally to the desired DP1000 microstructure.

During heat treatments, the variables being studied are temperature and time inside the laboratory furnace. All thermal treatments were carried out in preheated furnaces in the desired temperatures. During introduction of the specimen inside the furnace, a temperature drop is noticed. The desired temperature is, however, regained in couple of seconds. These seconds are very crucial, especially during intercritical annealing for short times, for instance 30 or 60 seconds. On the contrary, for longer times, such as 5, 10 or 60 minutes, retrieval time of the set temperature can be considered negligible, because specimens reach thermodynamic equilibrium and the final result does not change. For that reason, for short or intermediate intercritical annealing times, the timing starts when the laboratory furnace temperature reaches 10 or less Celsius degrees below the set temperature. Due to that temperature drop, the heating rate mode is adjusted suitably, so as to minimize the retrieval time of the desired temperature.

Table 3: The initial thermal treatment that was applied, prior to intercritical annealing.

Specimens	Step 1	Time	Step 2	Time	Step 3
All	Heating at 854°C	30 min	Heating at 550°C	60 min	Air Cooling (25°C)

Table 4: Naming and intercritical annealing holding times part a.

Specimens Name	Step 1	Time	Step 2
1	Heating at 700°C	30 seconds	Quenching
2	Heating at 700°C	1 minute	Quenching
3	Heating at 700°C	2 minutes	Quenching
4	Heating at 700°C	3 minutes	Quenching
5	Heating at 700°C	4 minutes	Quenching
6	Heating at 700°C	5 minutes	Quenching
7	Heating at 700°C	10 minutes	Quenching
8	Heating at 700°C	1 hour	Quenching
9	Heating at 720°C	30 seconds	Quenching
10	Heating at 720°C	1 minute	Quenching
11	Heating at 720°C	2 minutes	Quenching
12	Heating at 720°C	3 minutes	Quenching
13	Heating at 720°C	4 minutes	Quenching
14	Heating at 720°C	5 minutes	Quenching
15	Heating at 720°C	10 minutes	Quenching
16	Heating at 720°C	1 hour	Quenching

Table 5: Naming and intercritical annealing holding times part b.

Specimens	Step 1	Time	Step 2
17	Heating at 750°C	30 seconds	Quenching
18	Heating at 750°C	1 minute	Quenching
19	Heating at 750°C	2 minutes	Quenching
20	Heating at 750°C	3 minutes	Quenching
21	Heating at 750°C	4 minutes	Quenching
22	Heating at 750°C	5 minutes	Quenching
23	Heating at 750°C	10 minutes	Quenching
24	Heating at 750°C	1 hour	Quenching
25	Heating at 760°C	30 seconds	Quenching
26	Heating at 760°C	1 minute	Quenching
27	Heating at 760°C	2 minutes	Quenching
28	Heating at 760°C	3 minutes	Quenching
29	Heating at 760°C	4 minutes	Quenching
30	Heating at 760°C	5 minutes	Quenching
31	Heating at 760°C	10 minutes	Quenching
32	Heating at 760°C	1 hour	Quenching

Table 6: Naming and intercritical annealing holding times part c.

Specimens	Step 1	Time	Step 2
33	Heating at 770°C	30 seconds	Quenching
34	Heating at 770°C	1 minute	Quenching
35	Heating at 770°C	2 minutes	Quenching
36	Heating at 770°C	3 minutes	Quenching
37	Heating at 770°C	4 minutes	Quenching
38	Heating at 770°C	5 minutes	Quenching
39	Heating at 770°C	10 minutes	Quenching
40	Heating at 770°C	1 hour	Quenching
41	Heating at 780°C	30 seconds	Quenching
42	Heating at 780°C	1 minute	Quenching
43	Heating at 780°C	2 minutes	Quenching
44	Heating at 780°C	3 minutes	Quenching
45	Heating at 780°C	4 minutes	Quenching
46	Heating at 780°C	5 minutes	Quenching
47	Heating at 780°C	10 minutes	Quenching
48	Heating at 780°C	1 hour	Quenching

4. Metallography

After the heat treatment, each specimen was grinded with the proper SiC grinding papers in order to remove the thermal oxidation film that was produced during the heat treatment and create a plane and smooth surface. The grinding papers that were used were 80, 180, 320, 500, 800 and 1000 grid. In order to erase lines that occurred during grinding, specimen's direction in the grinding machine was changed by 90 degrees after every grid.

Grinding is followed by polishing. For this step, a diamond paste was used, with grain size 3 μm that was spread on the fabric discs of the polishing machine. As a result, a smooth surface is produced. In

order to create an ultra smooth, a second polishing step was applied. For that purpose, a 0.3 μm alumina powder was spread on the proper fabric disc of the polishing machine. The specimens were not placed in a resin, as usual, and for that reason grinding and polishing were performed with double sided tape. The result was a smooth mirror-like surface. To create a contrast between the existing phases of DP1000, each specimen was chemical etched with a two-stage etching technique. This technique was proposed by Vander Voort [28] and it consists of initial etching with Nital:

(a) Nital 2% (2ml HNO_3 in 98ml ethanol) for 1-2 seconds followed by

(b) aquatic solution Sodium Metabisulfite 10% (10g $Na_2S_2O_5$ in 100ml distilled water) for 20 seconds.

After each step, each specimen was rinsed with water and washed out with ethanol, once or twice and then was dried under a warm air flow.

Finally, all specimens were observed with an optical microscope Leica DLM and micrographs were obtained with a Canon EOS 600D.

5. Image Analysis

For each individual specimen, 3 sub regions were photographed with the Canon EOS 600D camera. These regions are along the rolling direction (L-dimension), as presented in Figure 3 (labeling scheme). In each region two pictures are taken; one for microscope magnification x500 and one for x1000 magnification. Consequently, there are six different pictures of each specimen.

All metallographic photos were edited via Image J software. The volume fraction of martensite (and austenite) the different annealing routes in the water-quenched specimens was determined by automatic counting techniques with the use of Image J software. This percentage was calculated as the average value of martensite between the six pictures of each specimen.

Photo editing took place with the software Image J. In the selected photos, appropriate filters were applied in order to create color contrast between the two phases. Light and dark regions represent the ferritic and martensitic regions respectively. This match is based on the used chemical reagents Nital and Metabisulfite. According to Vander Voort [28], Metabisulfite darkens areas of martensite, while the initially used Nital colors with light dark color the grain boundaries. Attention must be paid in the usage of these reagents, as it can drive to overetching or underetching phenomena in the specimen surface. Consequently, chemical etching is a subjective process and is based on the trial and error method. Moreover, subjective process is also the process of the limit selection during the threshold command of the Image J program. For that reason, an error of the order of 5% is considered (±5% from the actual phase percentage). In any case, martensite volume fraction must not exceed the value set from the thermodynamic equilibrium, which is calculated via the ThermoCalc software.

6. Microhardness evaluation

Following the metallographic analysis, the micro hardness of all specimens was measured. Generally, hardness is defined as the property of a material to resist to the penetration of another, harder

material. At first, a polishing step is required, in order to erase the previous chemical etching and create a new mirror like surface. A Woolpert Vickers microhardness tester was used. For the measurements a diamond penetrator with regular square pyramid shape was used. The penetrator leaves on the specimen surface a rhombical trace with d_1 and d_2 diagonals. Micro hardness tests were carried out with a 300 gram (0.3 kg) load. The two diagonals of the rhomb are measured giving the final value of the micro hardness in Vickers scale (HV) according to the following formula: $HV = F/A = 1.854*F/d^2$, where F is the imposed load, A the trace surface area and $d = (d_1 + d_2) / 2$ (average diagonal value).

An average of 20 measurements was performed for each specimen and an average value was calculated.

7. Thermo-Calc

Thermodynamic calculations of the proposed chemical composition mentioned in Table 1, were performed with Thermo-Calc and TCFE6 database in order to evaluate the phase diagram of the material, the temperature at which austenite begins to form during heating (Ac_1), the temperature at which the transformation of ferrite to austenite is completed during heating (Ac_3) as well as the phase fractions during the intercritical annealing process.

Kinetic calculations were performed with the diffusion software DICTRA during work for RFCS TOOLKIT project [25]. These results are presented in the project report, but some will be referenced in the current work. These referred modeling results are very useful as they constitute the basis for the comparison with the experimental data from the current work.

Chapter 4: Results

1. Metallographic analysis

The results of the metallograpic analysis are presented in this chapter of the present work. The initial thermal treatment that was applied as described in Table 3, prior to intercritical annealing, consists of heating in the full austenitic zone (854^{o}C), for 30 minutes and then isothermal holding at 550^{o}C, in the pearlitic region, for 60 minutes and finally air cooling. This heat treatment had as a result a ferrite-pearlite microstructure. This initial step was performed in order to eliminate the original ultra fine grain size and create a new microstructure with greater and more distinct grains to be observed in the optical microscope. A metallography of the initial microstructure is presented in Figure 4. This specimen exhibits a ferritic-pearlitic microstructure. As the carbon content of the alloy is very low the microstructure is mainly ferritic (light grains). The microstructure was revealed by etching with a 2% Nital reagent as proposed by Van der Voort [28].

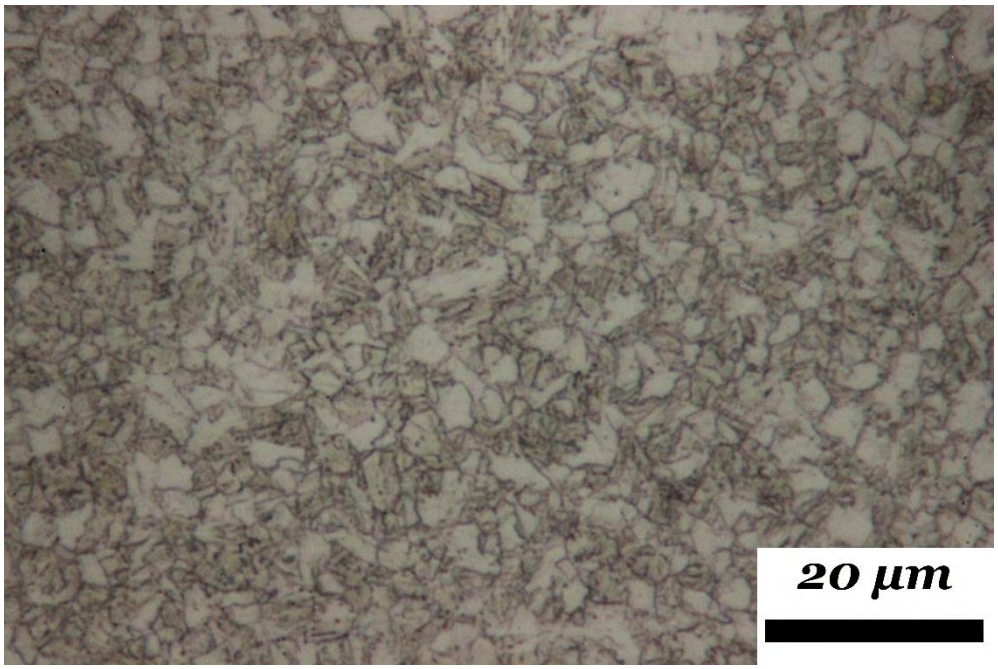

Figure 4: Metallography of a specimen heated in the full austenitic zone at 854^{o}C for 30 minutes followed by isothermal holding at 550^{o}C for 60 minutes and finally air cooling. (Magnification x1000)

As mentioned in the experimental procedure, 6 areas were photographed for each individual specimen, but in this chapter, only one representative micrograph for each specimen is presented. The micrographs are all in the x1000 magnification. Light (light yellow) and dark (dark brown) regions represent the ferritic and martensitic phases respectively [28].

The lowest intercritical annealing temperature that was selected is 700^{o}C. Micrographs for varying holding times at 700^{o}C are presented in Figure 5. Magnification of all images is x1000 and holding time starts from 30sec up to 1 hour. In Figure 5 (a) the specimen subjected to IA heat treatment for

30sec is depicted. Light yellow grains are observed along with the grain boundaries. These grains correspond to ferrite. Some very minute areas in between the triple points of the ferrite grain boundaries are observed, but they are very fine and few. The isothermal temperature is quite low and the isothermal holding time too short, so very little if any austenite was formed during IA at 700^{o}C. Subsequently no martensite is evident after quenching from this temperature. Figure 5 (b) depicts the specimen subjected to IA heat treatment for 60sec. Light yellow grains are observed again along with the grain boundaries. These grains correspond to ferrite. For 60sec holding time a dispersion of small dark grains is observed at the triple points of the ferrite grain boundaries. It is obvious that they are more easily distinguished than in the case of the 30sec holding time. These dark grains represent martensite formed from prior austenite during quenching from the IA region. As holding time progresses in Figure 5 (c) to 2min a similar scenario is observed with light yellow ferrite grain and dark brown martensite grains. Martensite grains are larger than for 60sec IA holding time but still quite small and isolated by the larger ferrite grains. Holding time of 3min at 700^{o}C in Figure 5 (d) produces even larger martensite grains growing intergranular to the the ferrite grains. Larger holding time by only 1min at 4min in Figure 5 (e) results in a more prominent change of the martensite phase as the smaller intergranular grains have grown and connected with each other, isolating larger ferrite grains. Holding time of 5min in Figure 5 (f) presents a similar behavior with connected larger martensite grains and isolated large ferrite grains. Figure 5 (g) and (h) depict micrographs for IA holding time 10 min and 1hour respectively, these micrographs exhibit similar behavior as in the case of 5min. The volume fraction of the respective phase is presented later after image analysis measurements

By observing the overall heat treatment, it is obvious that the average grain size of ferrite varies from micrograph to micrograph, this derives from the fact that over the surface of the specimens there are areas with different average grain size. The specimen with the shortest holding time is 30 seconds shows almost entirely a ferrite structure with very small dark areas which are uncertain if it is martensite or pearlite that could not dissolve or both. Proceeding to two and four minutes it is observed that although the overall volume fraction of martensite has grown over time it exhibits a different shape than in the case of 1 and 3 minutes. In this case martensite is not formed in the shape of equiaxed grains but in a plate shape. This difference in shape could be attributed in the ferrite grain size for each case. The ferrite grain size in the case of 2 and 4 minutes is much larger than those of 1 and 3 minutes.

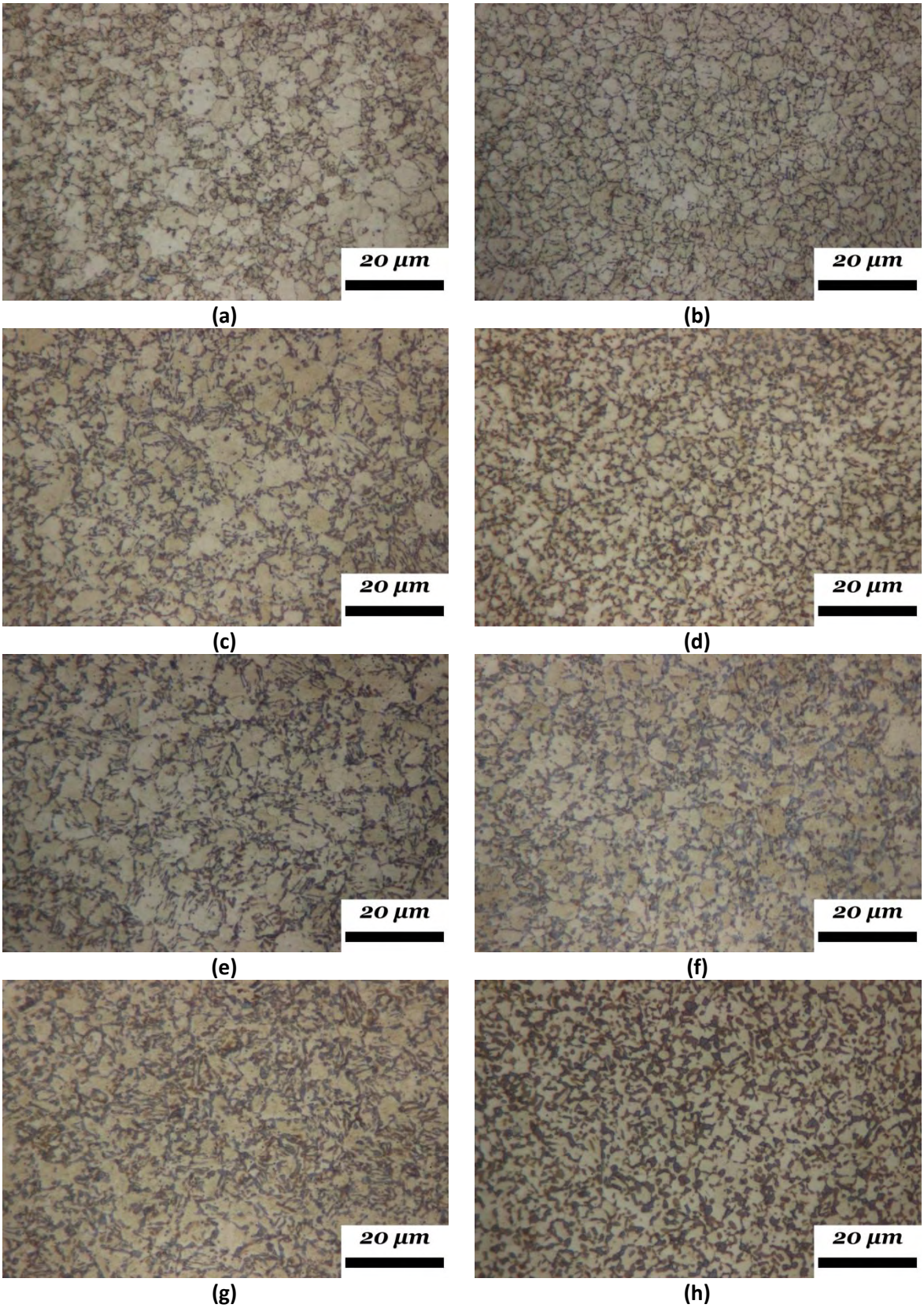

Figure 5: Intercritical annealing at 700°C for varying times 0.5 min (a), 1 min (b), 2 min (c), 3 min (d), 4 min (e), 5min (f), 10min (g), and 1 hour (h). Magnification of all images is x1000

The second intercritical annealing temperature that was selected is 720^{o}C. Micrographs for varying holding times at 720^{o}C are presented in Figure 6. In Figure 6 (a) the specimen subjected to IA heat treatment for 30sec is depicted. Light yellow grains are observed along with the grain boundaries. These grains correspond to ferrite. The average grain size of ferrite varies over the surface of the specimens. Some very minute areas in between the triple points of the ferrite grain boundaries are observed, but they could either martensite or pearlite or both. The isothermal temperature is quite low and the isothermal holding time too short, so very little if any austenite was formed during IA at 720^{o}C. Figure 6 (b) depicts the specimen subjected to IA heat treatment for 60sec. Light yellow grains are observed again along with the grain boundaries. These grains correspond to ferrite. For 60sec holding time a dispersion of small dark grains is observed at the triple points of the ferrite grain boundaries. It is obvious that they are more easily distinguished than in the case of the 30sec holding time. These dark grains represent martensite formed from prior austenite during quenching from the IA region. As holding time progresses in Figure 6 (c) to 2min a similar scenario is observed with light yellow ferrite grain and dark brown martensite grains. Martensite grains are larger than for 60sec IA holding time but steel quite small and isolated by the larger ferrite grains. Holding time of 3min at 720^{o}C in Figure 6 (d) produces even larger martensite grains growing intergranular to the the ferrite grains. Larger holding time by only 1min at 4min in Figure 6 (e) results in a more prominent change of the martensite phase as the smaller intergranular grains have grown and connected with each other, isolating larger ferrite grains. Holding time of 5min in Figure 6 (f) presents a similar behavior with connected larger martensite grains and isolated large ferrite grains. Figure 6 (g) and (h) depict micrographs for IA holding time 10 min and 1hour respectively, these micrographs exhibit similar behavior as in the case of 5min. The volume fraction of the respective phase is presented later after image analysis measurements

The average grain size of ferrite varies from micrograph to micrograph, as was evident in the case of IA holding at 700^{o}C. Similar behavior with two different shapes of martensite (equiaxed vs plate like martensite) present is also observed for IA at 720^{o}C.

Overall for corresponding times more martensite is formed in the case of IA at 720^{o}C than at 700^{o}C.

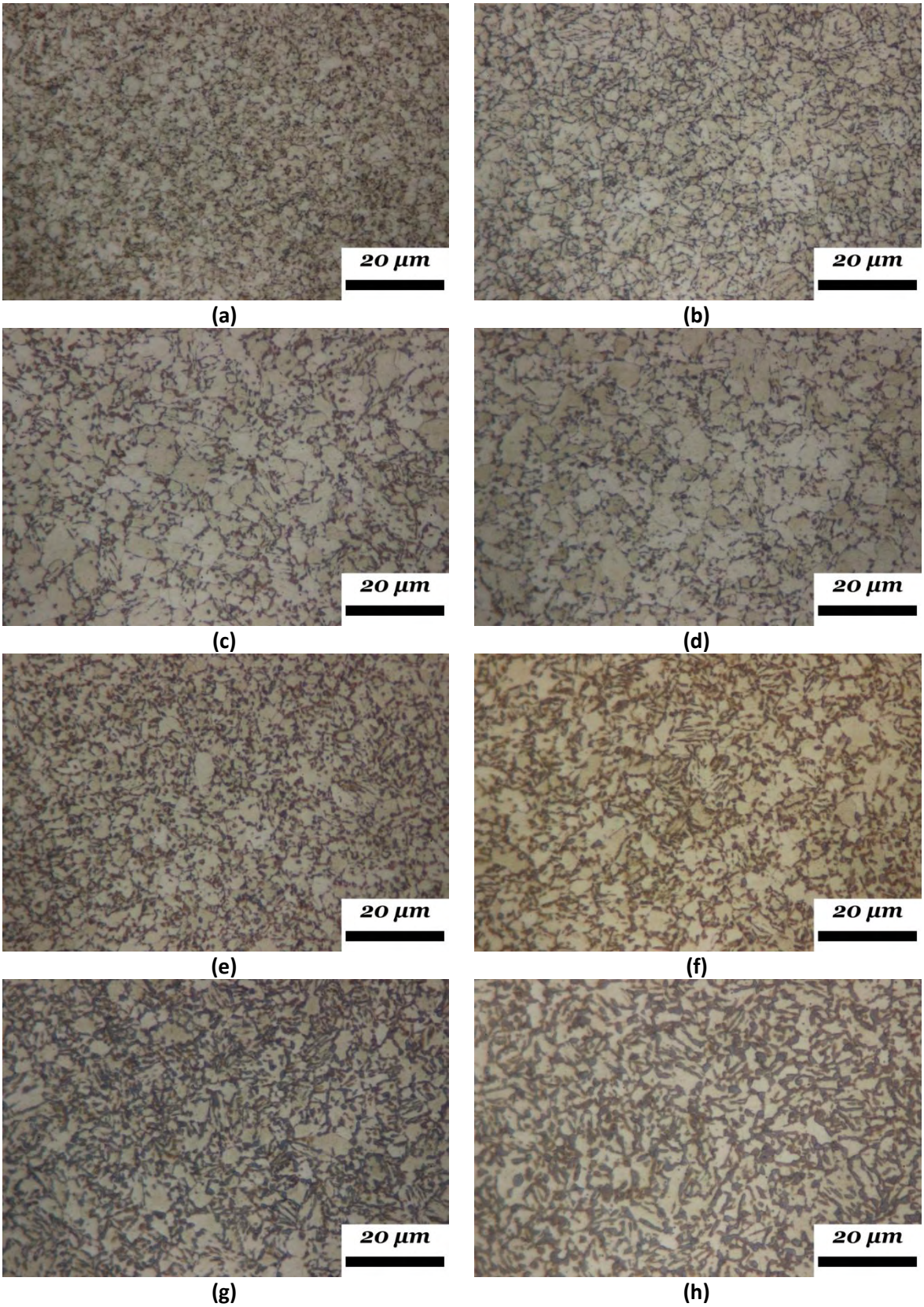

Figure 6: Intercritical annealing at 720°C for varying times 0.5 min (a), 1 min (b), 2 min (c), 3 min (d), 4 min (e), 5min (f), 10min (g), and 1 hour (h). Magnification of all images is x1000

Micrographs for varying holding times at 750^{o}C are presented in Figure 7. Magnification of all images is x1000 and holding time starts from 30sec up to 1 hour. In Figure 7 (a) the specimen subjected to IA heat treatment for 30sec is depicted. Yellow grains are observed along with the grain boundaries. These grains correspond to ferrite. Some darker areas could correspond to either pearlite or martensite. The isothermal temperature is in the medium region and the overall kinetics of transformations is different than it was in the previous cases of lower temperatures (700^{o}C and 720^{o}C). Figure 7 (b) depicts the specimen subjected to IA heat treatment for 60sec. Light yellow grains are observed again along with the grain boundaries. These grains correspond to ferrite. For 60sec holding time a dispersion of small dark grains is observed at the triple points of the ferrite grain boundaries. These dark grains represent martensite formed from prior austenite during quenching from the IA region. As holding time progresses in Figure 7 (c) to 2min a similar scenario is observed with light yellow ferrite grain and dark brown martensite grains. Martensite grains are larger than for 60sec IA holding time but still quite small and isolated by the larger ferrite grains. Holding time of 3min at 750^{o}C in Figure 7 (d) produces even larger martensite grains growing intergranular to the ferrite grains. Larger holding time by only 1min at 4min in Figure 7 (e) results in a more prominent change of the martensite phase as the smaller intergranular grains have grown and connected with each other, isolating larger ferrite grains. Holding time of 5min in Figure 7 (f) presents a similar behavior with connected larger martensite grains and isolated large ferrite grains. Figure 7 (g) and Figure 7 (h) depict micrographs for IA holding time 10 min and 1hour respectively, these micrographs exhibit similar behavior as in the case of 5min. The volume fraction of the respective phase is presented later after image analysis measurements

The average grain size of ferrite varies from micrograph to micrograph, as was evident in the case of IA holding at 700^{o}C and 720^{o}C. Similar behavior with two different shapes of martensite (equiaxed vs plate like martensite) present is also observed for IA at 750^{o}C.

Overall for corresponding times more martensite is formed in the case of IA at 750^{o}C than at 720^{o}C and 700^{o}C.

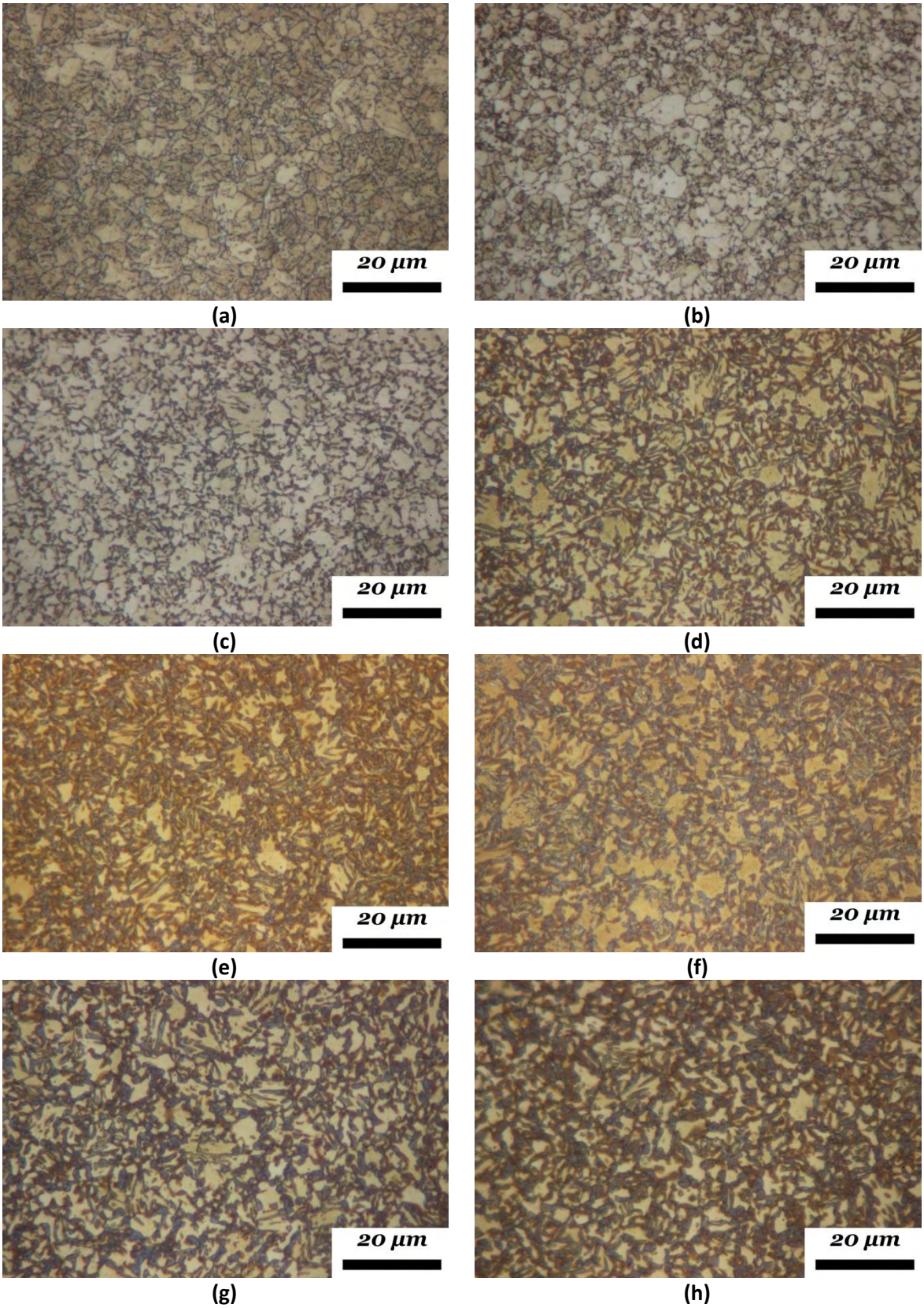

Figure 7: Intercritical annealing at 750°C for varying times 0.5 min (a), 1 min (b), 2 min (c), 3 min (d), 4 min (e), 5min (f), 10min (g), and 1 hour (h). Magnification of all images is x1000

Micrographs for varying holding times at 760^{o}C are presented in Figure 8. Magnification of all images is x1000 and holding time starts from 30sec up to 1 hour. In Figure 8 (a) the specimen subjected to IA heat treatment for 30sec is depicted. Light yellow grains are observed along with the grain boundaries. These grains correspond to ferrite. Some very minute areas in between the triple points of the ferrite grain boundaries are observed, but they are very fine and few. Figure 8 (b) depicts the specimen subjected to IA heat treatment for 60sec. Light yellow grains are observed again along with the grain boundaries. These grains correspond to ferrite. For 60sec holding time a dispersion of small dark grains is observed at the triple points of the ferrite grain boundaries. It is obvious that they are more easily distinguished than in the case of the 30sec holding time. These dark grains represent martensite formed from prior austenite during quenching from the IA region. As holding time progresses in Figure 8 (c) to 2min a similar scenario is observed with light yellow ferrite grain and dark brown martensite grains. Martensite grains are larger than for 60sec IA holding time but still quite small and isolated by the larger ferrite grains. As far as the metallographic examination of IA at 760^{o}C is concerned specimen up to 2 min IA time exhibit similar behavior with specimen subjected to IA at lower temperatures. For intermediate times 3 to 10 min it proved quite cumbersome to study these specimens metallographically. It is speculated that isothermal temperature of 760^{o}C is in the high region of IA temperatures and the overall kinetics of transformations is different than it was in the previous cases of lower temperatures (700^{o}C and 720^{o}C), thus the element partitioning in each phase especially martensite can be very different than in lower temperatures. This fact can inhibit phase etching with the normal etching routine. Holding time of 3min at 760^{o}C in Figure 8 (d) produces even larger martensite grains growing intergranular to the ferrite grains. Larger holding times at 4min in Figure 8 (e), 5min in Figure 8 (f) and 10 min in Figure 8 (g) depict micrographs that present similar behavior with connected larger martensite grains and isolated large ferrite grains. Finally holding time of 1 hour is presented in Figure 8 (h). The volume fraction of the respective phase is presented later after image analysis measurements

The average grain size of ferrite varies from micrograph to micrograph, as was evident in the case of IA holding at 700^{o}C and 720^{o}C. In this case the holding temperature of 760^{o}C is quite high so that a lot more martensite forms than at lower temperatures, so it is not easy to distinguish differences in shape of martensite (equiaxed vs plate like martensite) depending on grain size of ferrite.

Overall for corresponding times more martensite is formed in the case of IA at 760^{o}C than at 750^{o}C.

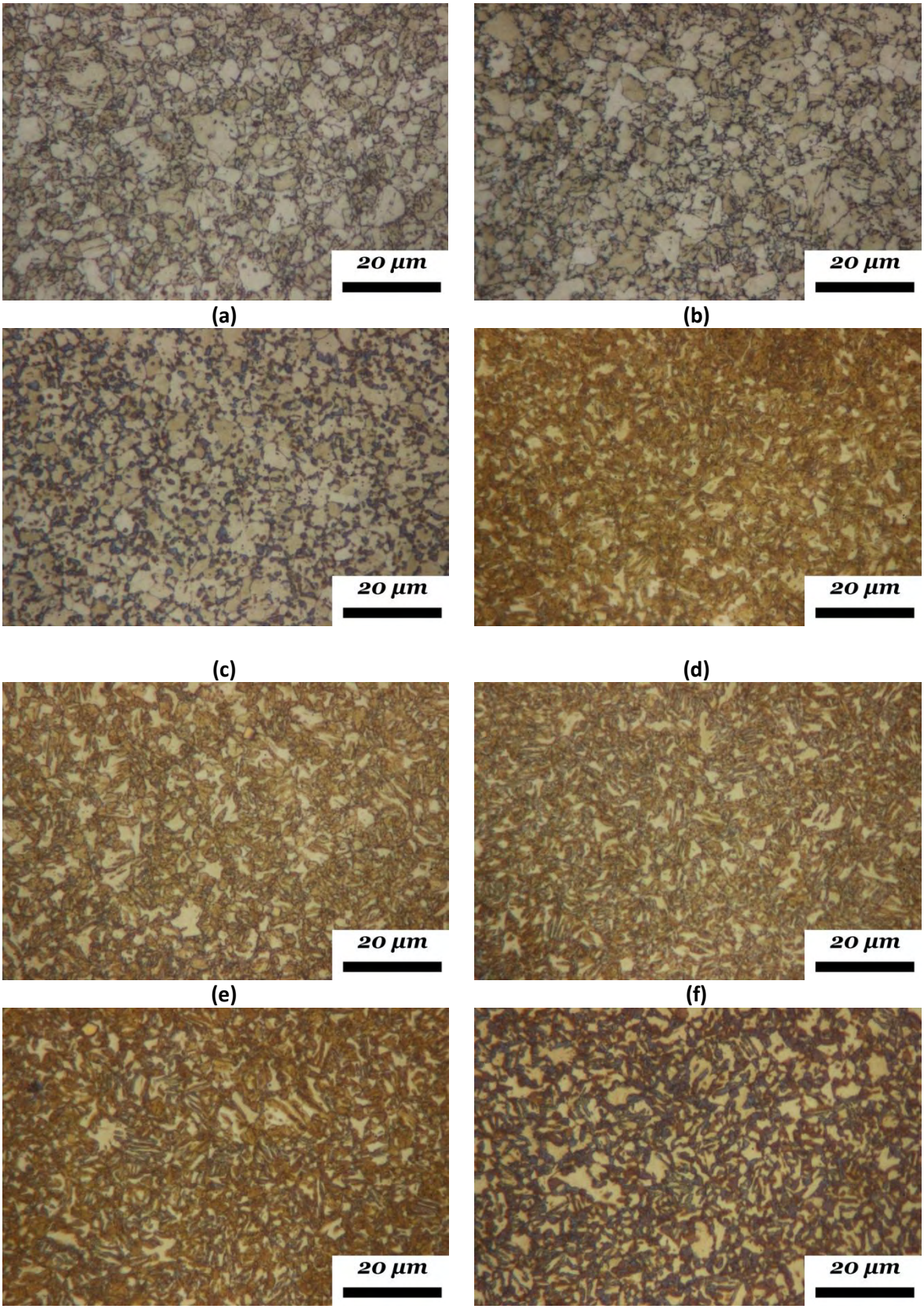

Figure 8: Intercritical annealing at 760°C for varying times 0.5 min (a), 1 min (b), 2 min (c), 3 min (d), 4 min (e), 5min (f), 10min (g), and 1 hour (h). Magnification of all images is x1000.

Micrographs for varying holding times at 770^{o}C are presented in Figure 9. Magnification of all images is x1000 and holding time starts from 30sec up to 1 hour. In Figure 9 (a) the specimen subjected to IA heat treatment for 30sec is depicted. Light yellow grains are observed along with the grain boundaries. These grains correspond to ferrite. Some very minute areas in between the triple points of the ferrite grain boundaries are observed. Figure 9 (b) depicts the specimen subjected to IA heat treatment for 60sec. Light yellow grains are observed again along with the grain boundaries. These grains correspond to ferrite. For 60sec holding time a dispersion of small dark grains is observed at the triple points of the ferrite grain boundaries. These dark grains represent martensite formed from prior austenite during quenching from the IA region. As holding time progresses in Figure 9 (c) to 2min a similar scenario is observed with light yellow ferrite grain and dark brown martensite grains. Martensite grains are a lot larger than for 60sec. As far as the metallographic examination for IA at 770^{o}C is concerned specimen up to 2 min IA time exhibit similar behavior with specimen subjected to IA at lower temperatures. For intermediate times 3 to 10 min it proved almost impossible to study these specimens metallographically. Specially to provide contrast between the two phases ferrite and martensite. It is speculated that isothermal temperature of 770^{o}C is in the high region of IA temperatures and the overall kinetics of transformations is different than it was in the previous cases of lower temperatures (700^{o}C and 720^{o}C), thus the element partitioning in each phase especially martensite can be very different than in lower temperatures. This fact can inhibit phase etching with the normal etching routine. Figure 9 (h) depicts a micrograph for IA holding time 1hour and the phase contrast is again apparent. The volume fraction of the respective phase is was not measured for this heat treatment.

Micrographs for varying holding times at 780^{o}C are presented in Figure 10. In Figure 10 (a) the specimen subjected to IA heat treatment for 30sec is depicted. Light yellow grains are observed along with the grain boundaries. These grains correspond to ferrite. Some very minute areas in between the triple points of the ferrite grain boundaries are observed. Figure 10 (b) depicts the specimen subjected to IA heat treatment for 60sec. Light yellow grains are observed again along with the grain boundaries. These grains correspond to ferrite. For 60sec holding time a dispersion of small dark grains is observed at the triple points of the ferrite grain boundaries. It is obvious that they are more easily distinguished than in the case of the 30sec holding time. These dark grains represent martensite formed from prior austenite during quenching from the IA region. As holding time progresses in Figure 10 (c) to 2min a similar scenario is observed with light yellow ferrite grain and dark brown martensite grains. Martensite grains are a lot larger than for 60sec IA holding time. As far as the metallographic examination for IA at 780^{o}C is concerned specimen up to 2 min IA time exhibit similar behavior with specimen subjected to IA at lower temperatures. For intermediate times 3 to 10 min it proved almost impossible to study these specimens metallographically. Specially to provide contrast between the two phases, ferrite and martensite. It is speculated that isothermal temperature of 780^{o}C is in the high region of IA temperatures and the overall kinetics of transformations is different than it was in the previous cases of lower temperatures (700^{o}C and 720^{o}C), thus the element partitioning in each phase especially martensite can be very different than in lower temperatures. This fact can inhibit phase etching with the normal etching routine. Figure 10 (h) depicts a micrograph for IA holding time 1hour and the phase contrast is again apparent. The volume fraction of the respective phase was not measured for this heat treatment.

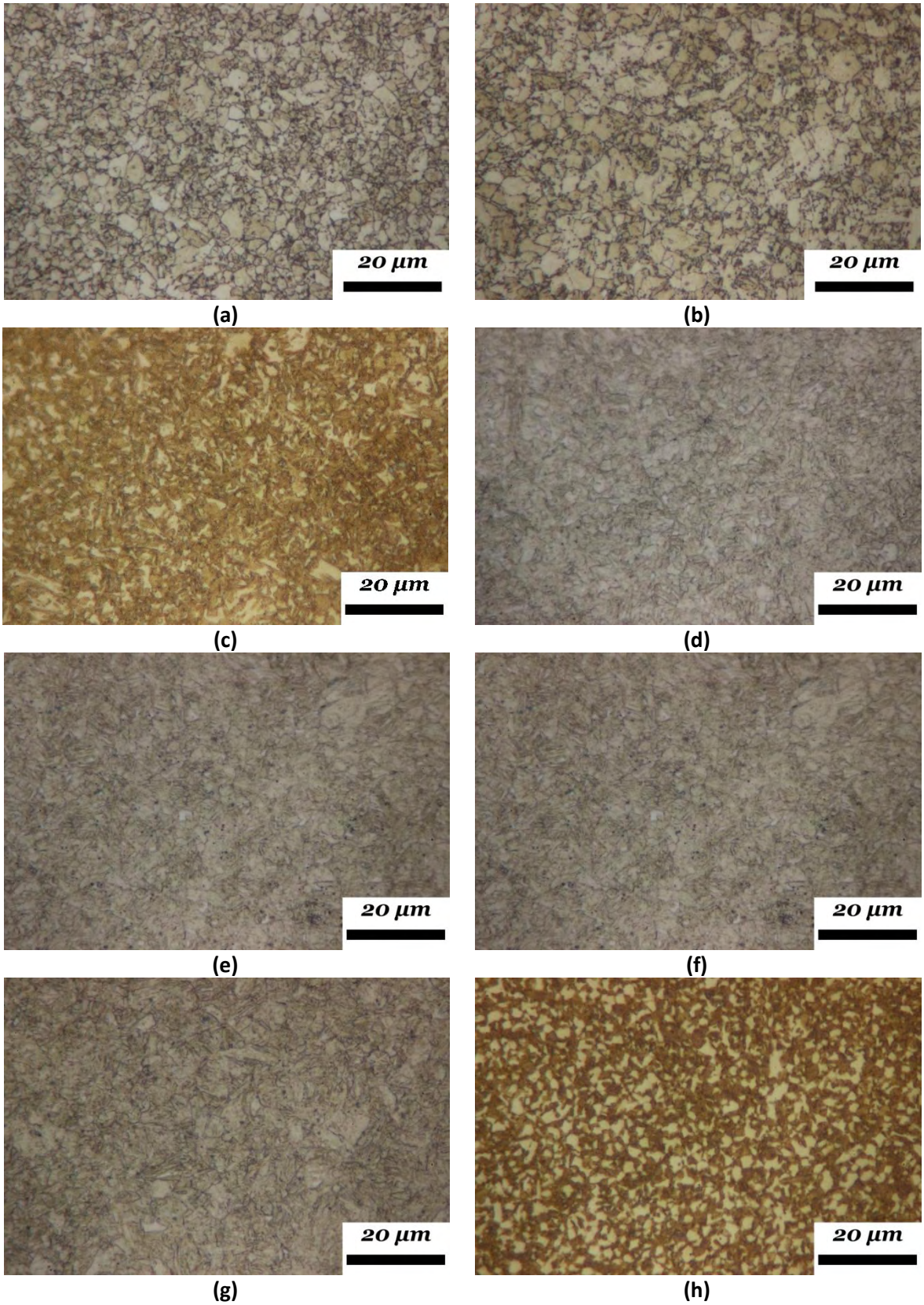

Figure 9: Intercritical annealing at 770°C for varying times 0.5 min (a), 1 min (b), 2 min (c), 5 min (d), 10 min (e) and 1 hour (f). Magnification of all images is x1000.

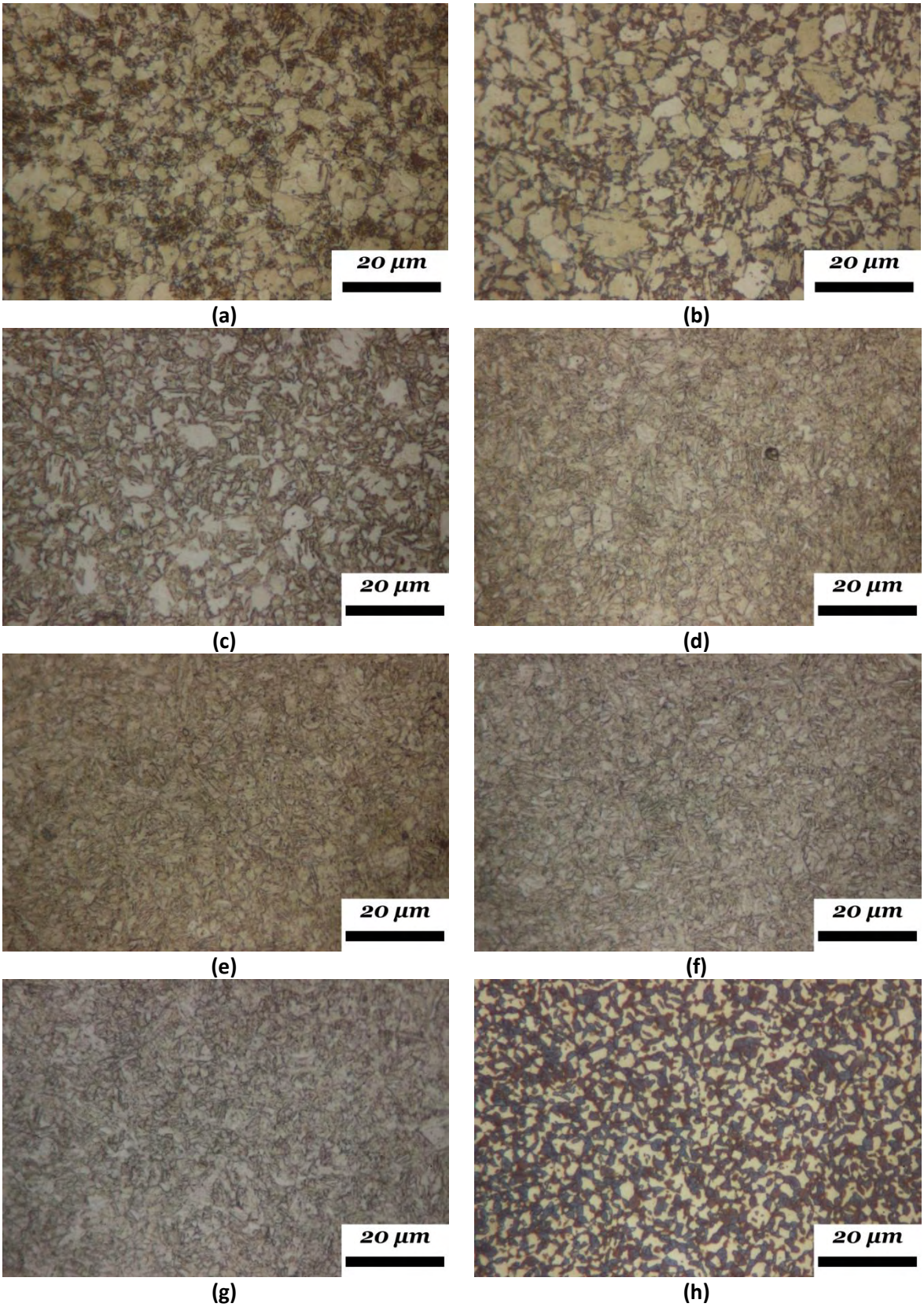

Figure 10: Intercritical annealing at 780°C for varying times 0.5 min (a), 1 min (b), 2 min (c), 5 min (d), 10 min (e) and 1 hour (f). Magnification of all images is x1000.

In Figure 11 to Figure 17 micrograph of intercritical annealing for a fixed holding time versus IA temperature are illustrated. For intercritical annealing for holding time 30sec Figure 11 for all IA temperatures a similar scenario is apparent ferrite grains (light yellow) with varying grain sizes are present, along with some very small areas in between the triple points of the ferrite grain boundaries. The isothermal holding time is too short, so these areas could be pearlite, martensite or both.

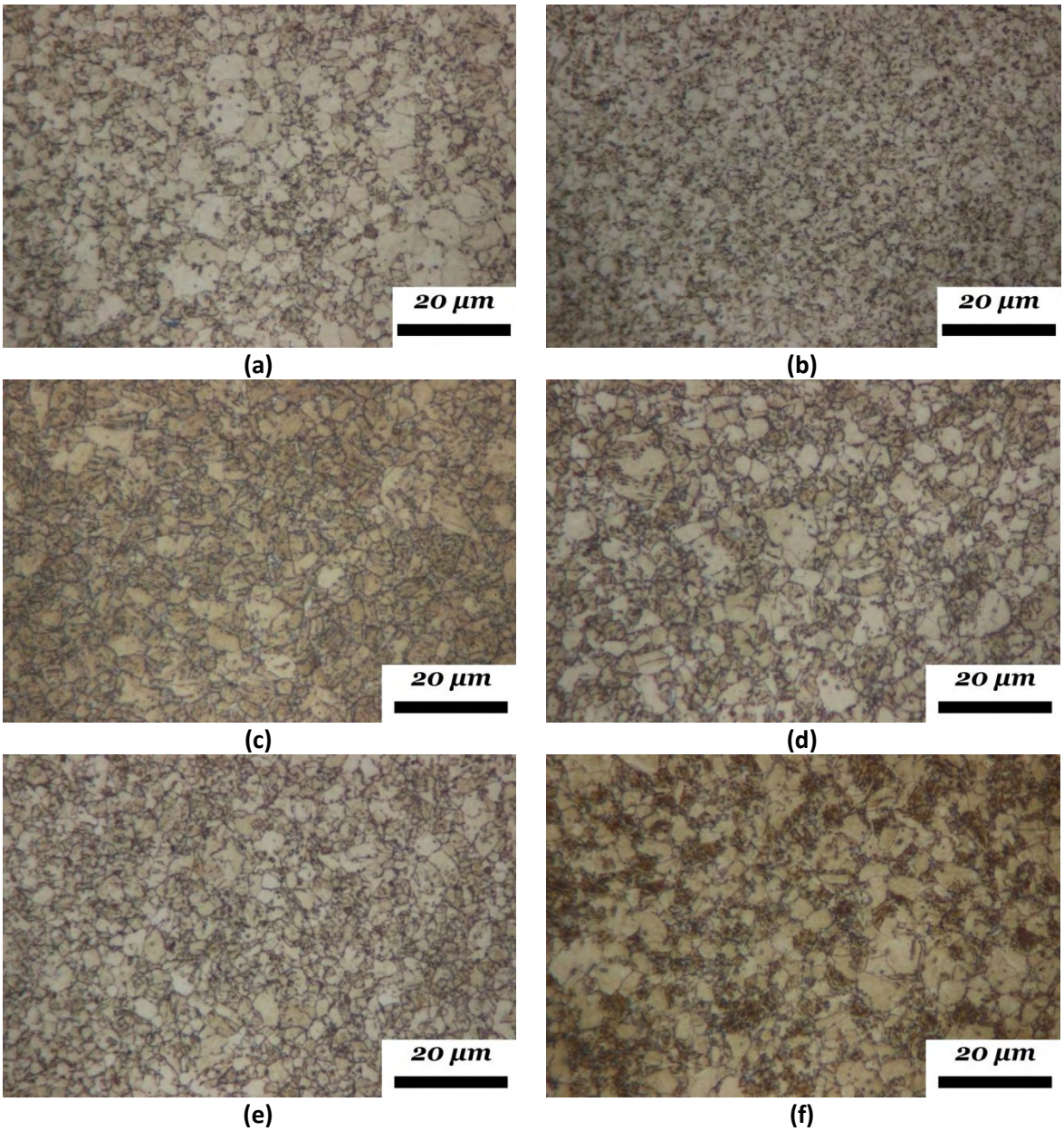

Figure 11: Intercritical annealing for 0.5 min for varying temperatures: 700°C (a), 720°C (b), 750°C (c), 760°C (d), 770°C (e) and 780°C (f). Magnification of all images is x1000.

In Figure 12 the micrographs of intercritical annealing for 60sec holding time versus IA temperature are illustrated. The evolution of martensite is clearer in this case. Ferrite grains (light yellow) with varying grain sizes are present, along with some very small areas in between the triple points of the ferrite grain boundaries. The isothermal holding time is short but it is evident that these areas are martensite, that grows into larger grains with higher IA temperature.

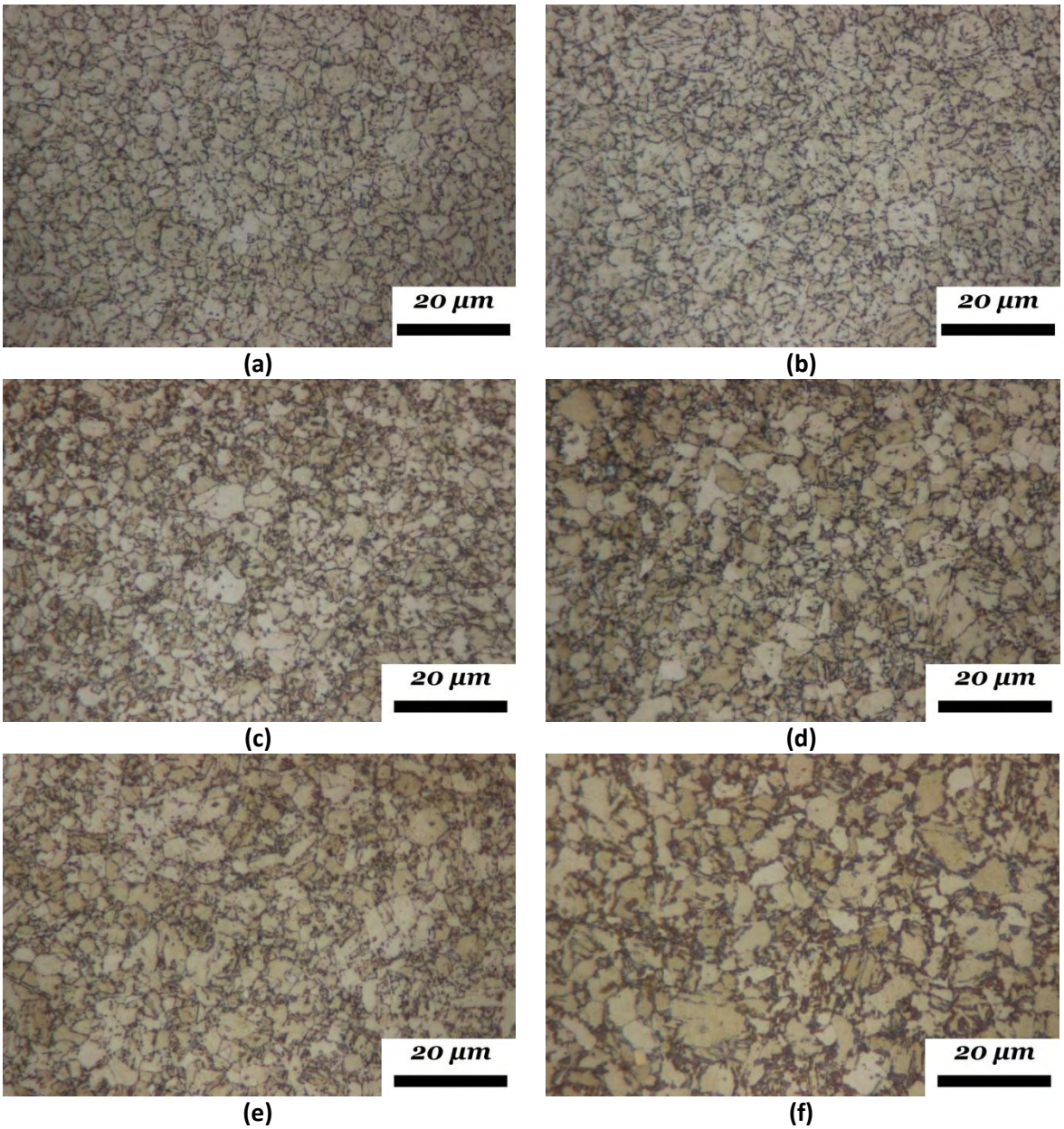

Figure 12: Intercritical annealing for 1 min for varying temperatures: 700°C (a), 720°C (b), 750°C (c), 760°C (d), 770°C (e) and 780°C (f). Magnification of all images is x1000.

Similarly, to 60sec of IA holding time in Figure 13 the micrographs of intercritical annealing for2min holding time versus IA temperature are illustrated. The evolution of martensite is clear. Ferrite grains (light yellow) with varying grain sizes are present, along with some very small areas (martensite) in between the triple points of the ferrite grain boundaries for IA temperatures up to 760^{o}C. Higher IA temperatures 770^{o}C and 780^{o}C produce very large martensite grains that amount to almost the equilibrium volume fraction of austenite during intercritical annealing.

Figure 14, Figure 15 and Figure 16 illustrate similar behavior for 3, 5 and 10 min holding time respectively the evolution of martensite is clear. Ferrite grains (light yellow) with varying grain sizes are present, along with some very small areas (martensite) in between the triple points of the ferrite grain boundaries for IA temperatures up to 760^{o}C. Higher IA temperatures 770^{o}C and 780^{o}C did not produce sufficient martensite ferrite phase contrast and were omitted.

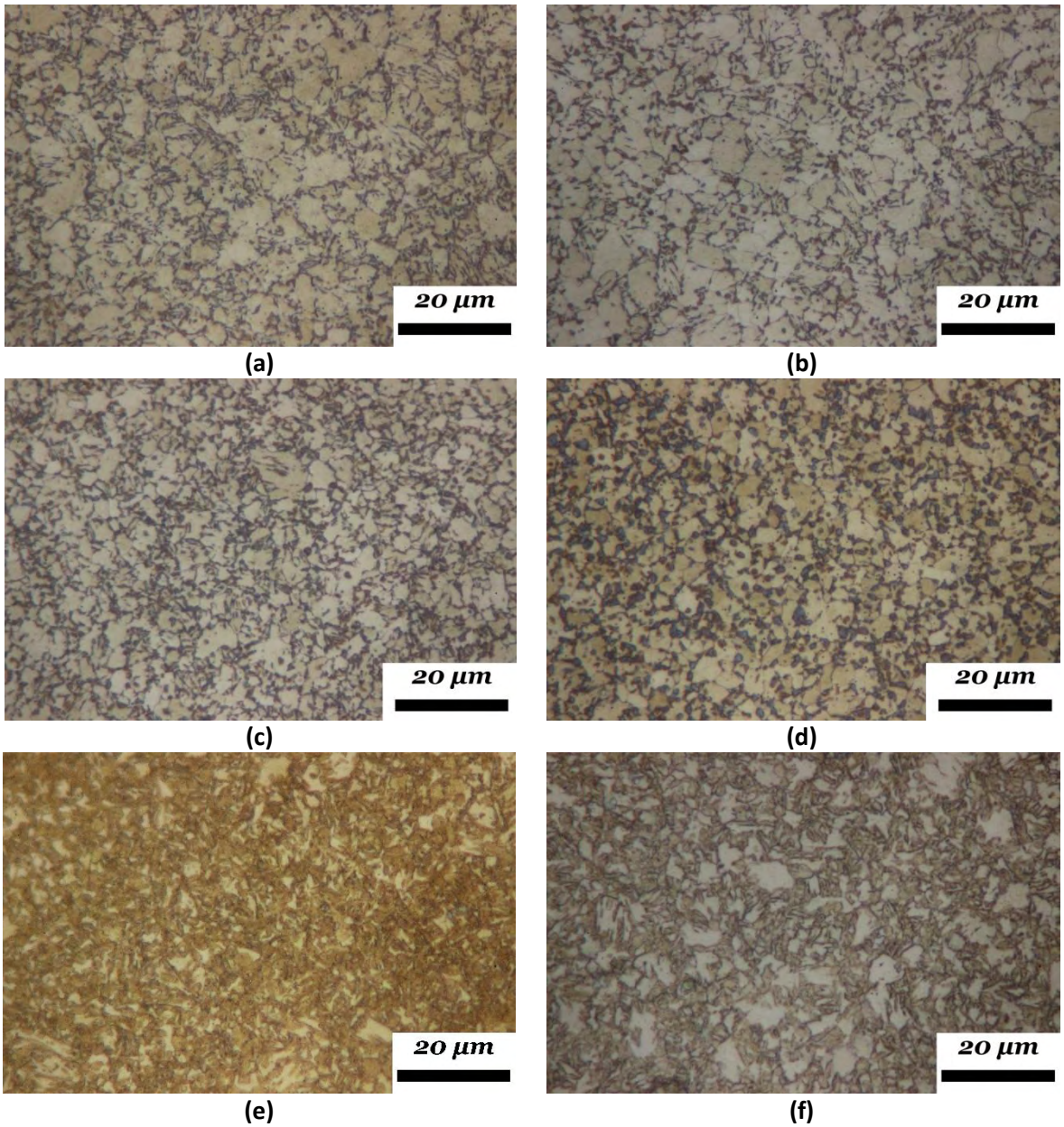

Figure 13: Intercritical annealing for 2 min for varying temperatures: 700^{o}C (a), 720^{o}C (b), 750^{o}C (c), 760^{o}C (d) and770^{o}C (e). Magnification of all images is x1000.

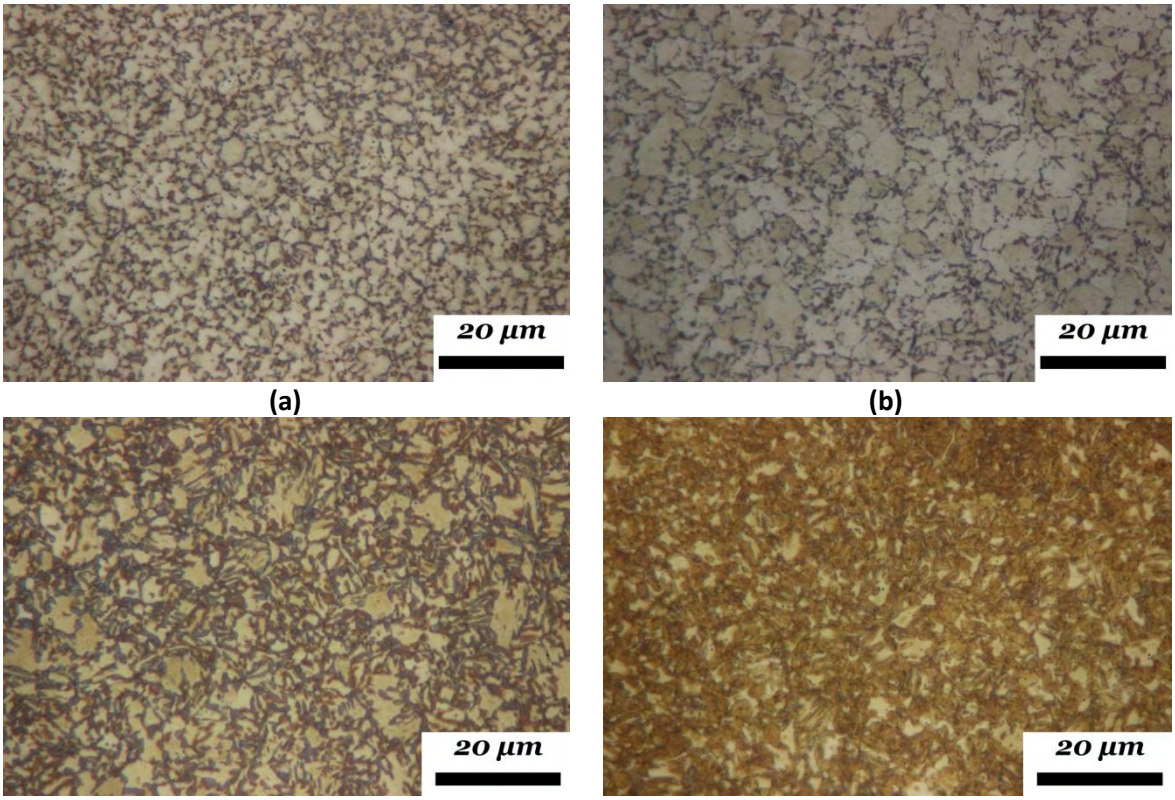

Figure 14: Intercritical annealing for 3 min for varying temperatures: 700°C (a), 720°C (b), 750°C (c) and 760°C (d). Magnification of all images is x1000.

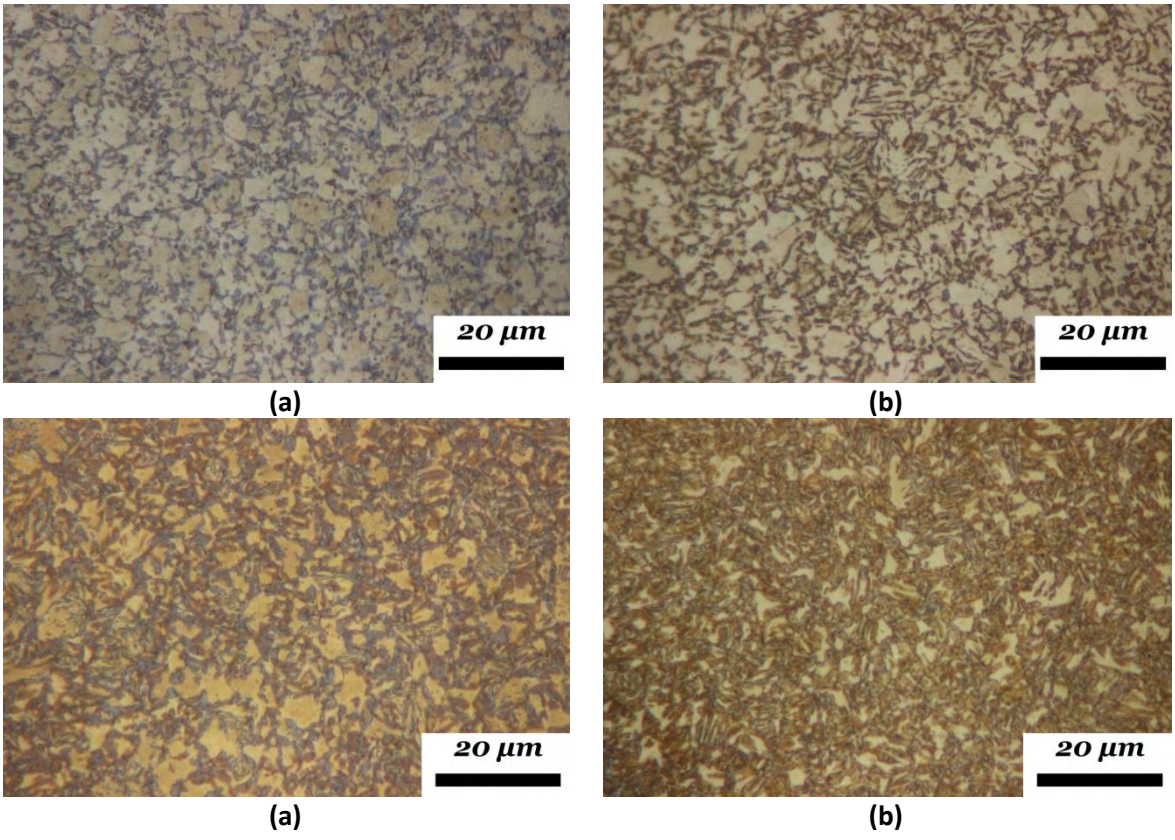

Figure 15: Intercritical annealing for 5 min for varying temperatures: 700°C (a), 720°C (b), 750°C (c) and 760°C. Magnification of all images is x1000.

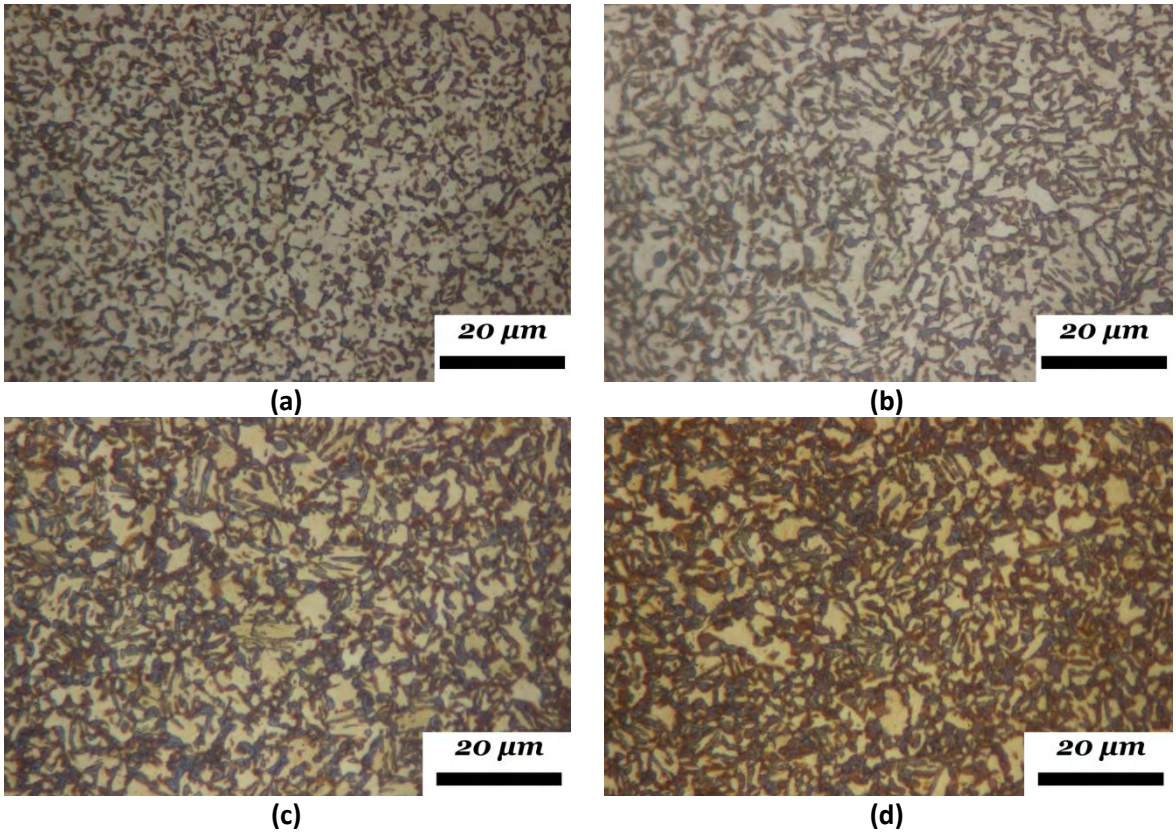

Figure 16: Intercritical annealing for 10 min for varying temperatures: 700°C (a), 720°C (b), 750°C (c), 760°C (d), 770°C (e) and 780°C (f). Magnification of all images is x1000.

Finally, in Figure 17 for 1 hour intercritical holding time the specimens are approaching equilibrium conditions and the evolution of martensite is again clear. Ferrite grains (light yellow), along with martensite (dark areas) for IA temperatures. The progressive evolution of martensite volume fraction with respect to IA temperature is evident. Higher IA temperatures 770°C and 780°C produce very large martensite grains that amount to almost the equilibrium volume fraction of austenite during intercritical annealing.

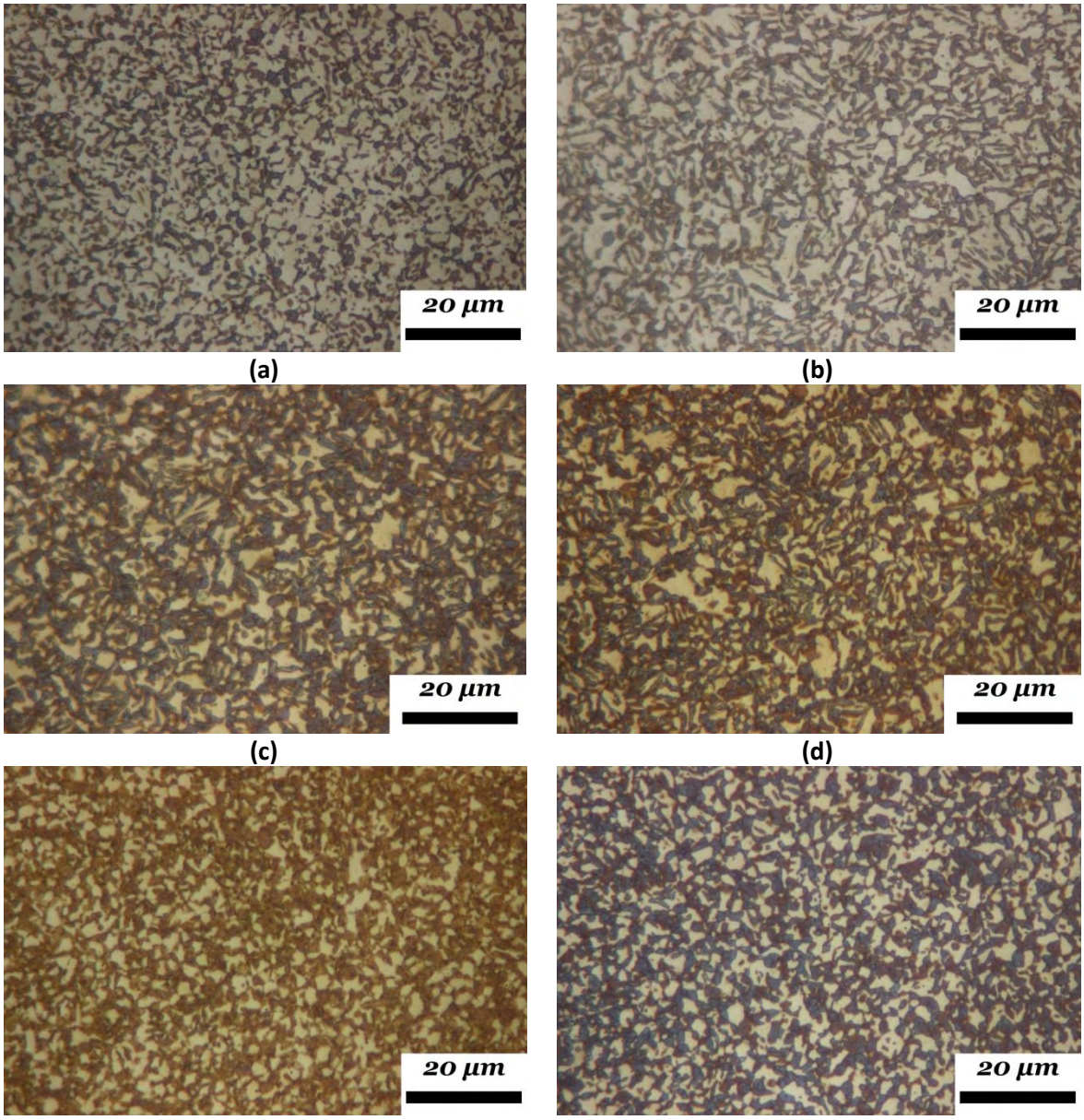

Figure 17: Intercritical annealing for 1 hour for varying temperatures: 700°C (a), 720°C (b), 750°C (c), 760°C (d), 770°C (e) and 780°C (f). Magnification of all images is x1000.

2. Image Analysis

The results of the image analysis are presented in this chapter. As mentioned in the experimental procedure the scientific software Image J was used for image processing and analysis. The micrographs analyzed are the same used for the metallographic analysis in the previous chapter. As already mentioned 6 areas were photographed for each individual specimen. One representative analyzed micrograph for each specimen is presented. The images are all in the x1000 magnification. After the appropriate image processing and filtering, the light regions (light gray) represent ferrite and the red regions martensite.

Images produced for image analysis for varying holding times at 700^{o}C are presented in Figure 18. Magnification of all images is x1000 and holding time starts from 30sec up to 1 hour. In Figure 18 (a) the specimen subjected to IA heat treatment for 30sec is depicted. Light gray grains are observed, and they correspond to ferrite. Some very small areas in the triple points of the ferrite grain boundaries are observed denoted with red color. Figure 18 (b) depicts the specimen subjected to IA heat treatment for 60sec. For 60sec holding time a dispersion of small red areas is observed at the triple points of the ferrite grain boundaries. It is obvious that they are more easily distinguished than in the case of the 30sec holding time. These red areas represent martensite formed from prior austenite during quenching from the IA region. As holding time progresses in Figure 18 (c) to 2min a similar microstructure is observed with light gray ferrite grain and red martensite grains. Martensite grains are larger than for 60sec IA holding time but still quite small and isolated by the larger ferrite grains. Holding time of 3min at 700^{o}C in Figure 18 (d) produces even larger martensite grains growing intergranular to the ferrite grains. Larger holding time at 4min in Figure 18 (e) results in a more prominent change of the martensite phase as the smaller intergranular grains have grown and connected with each other, isolating larger ferrite grains. Holding time of 5min in Figure 18 (f) presents a similar behavior with connected larger martensite grains and isolated large ferrite grains. Figure 18 (g) and (h) depict micrographs for IA holding time 10 min and 1hour respectively, these micrographs exhibit similar behavior as in the case of 5min. The volume fraction of the respective phases is presented in Table 7. Volume fraction of martensite for 30sec IA is measured at 5.5% and it acquires higher values as IA holding time increases. For 1 hour holding time it is measured at 22.51% equal to the volume fraction of austenite calculated with Thermocalc. There is always an error that should be considered when performing image analysis measurements. This error is in the range of ±5%. It should also be taken into account that for the two smaller holding times the experimental procedure could not be very precise.

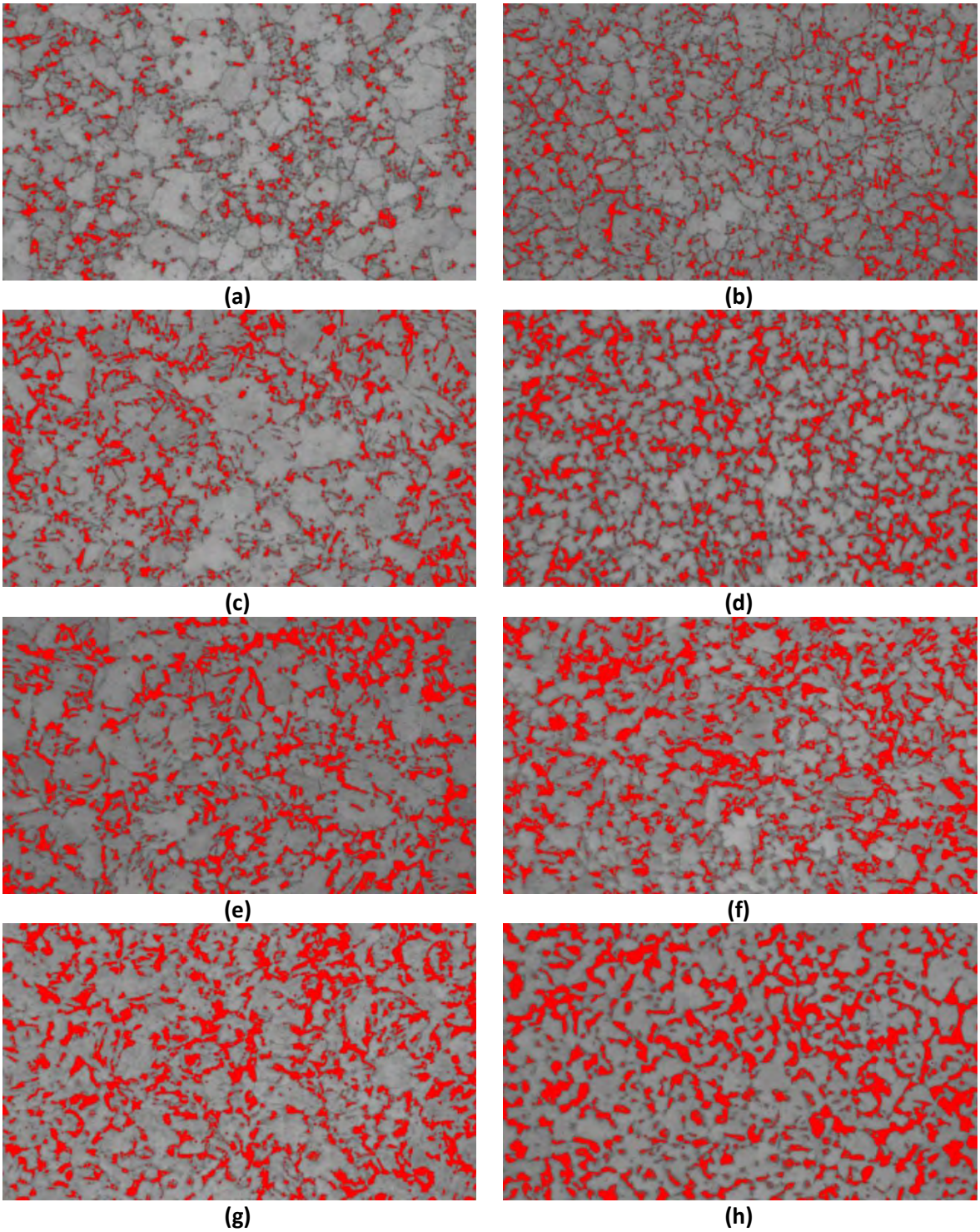

Figure 18: Intercritical annealing at 700°C for varying times 0.5 min (a), 1 min (b), 2 min (c), 3 min (d), 4 min (e) 5 min (f), 10 min (g) and 1 hour (h). Magnification of all images is x1000. The martensite volume fraction is noted in Table 7 below and is shown in all pictures in red.

Table 7: Volume fraction of martensite and ferrite with respect to IA holding time at 700°C.

Specimens (figure No)	Holding Time (min)	Volume Fraction Ferrite	Volume Fraction Martensite
a	**0.5**	94.48	5.52%
b	**1**	90.44	9.56%
c	**2**	87.43	12.57%
d	**3**	83.63	16.37%
e	**4**	81.46	18.54%
f	**5**	79.07	20.93%
g	**10**	78.21	21.79%
h	**60**	77.49	22.51%
Thermocalc		77.50	22.50%

Images produced for image analysis for varying holding times at 720°C are presented in Figure 19. Magnification of all images is x1000 and holding time starts from 30sec up to 1 hour. In Figure 19 (a) the specimen subjected to IA heat treatment for 30sec is depicted. Light gray grains are observed, and they correspond to ferrite. Some very small areas in the triple points of the ferrite grain boundaries are observed denoted with red color. Figure 19 (b) depicts the specimen subjected to IA heat treatment for 60sec. For 60sec holding time a dispersion of small red areas is observed at the triple points of the ferrite grain boundaries. It is obvious that they are more easily distinguished than in the case of the 30sec holding time. As holding time progresses in Figure 19 (c) to 2min a similar microstructure is observed with light gray ferrite grain and red martensite grains. Martensite grains are larger than for 60sec IA holding time but still quite small and isolated by the larger ferrite grains. Holding time of 3min at 720°C in Figure 19 (d) produces even larger martensite grains growing intergranular to the ferrite grains. Larger holding time by only 1min at 4min in Figure 19 (e) results in a more prominent change of the martensite phase as the smaller intergranular grains have grown and connected with each other, isolating larger ferrite grains. Holding time of 5min in Figure 19 (f) presents a similar behavior with connected larger martensite grains and isolated large ferrite grains. Figure 19 (g) and (h) depict micrographs for IA holding time 10 min and 1hour respectively, these micrographs exhibit similar behavior as in the case of 5min. The volume fraction of the respective phases are presented in Table 8. Volume fraction of martensite for 30sec IA is measured at 7.51% and it acquires higher values as IA holding time increases. For 1 hour holding time it is measured at 29.23% equal to the volume fraction of austenite calculated with Thermocalc.

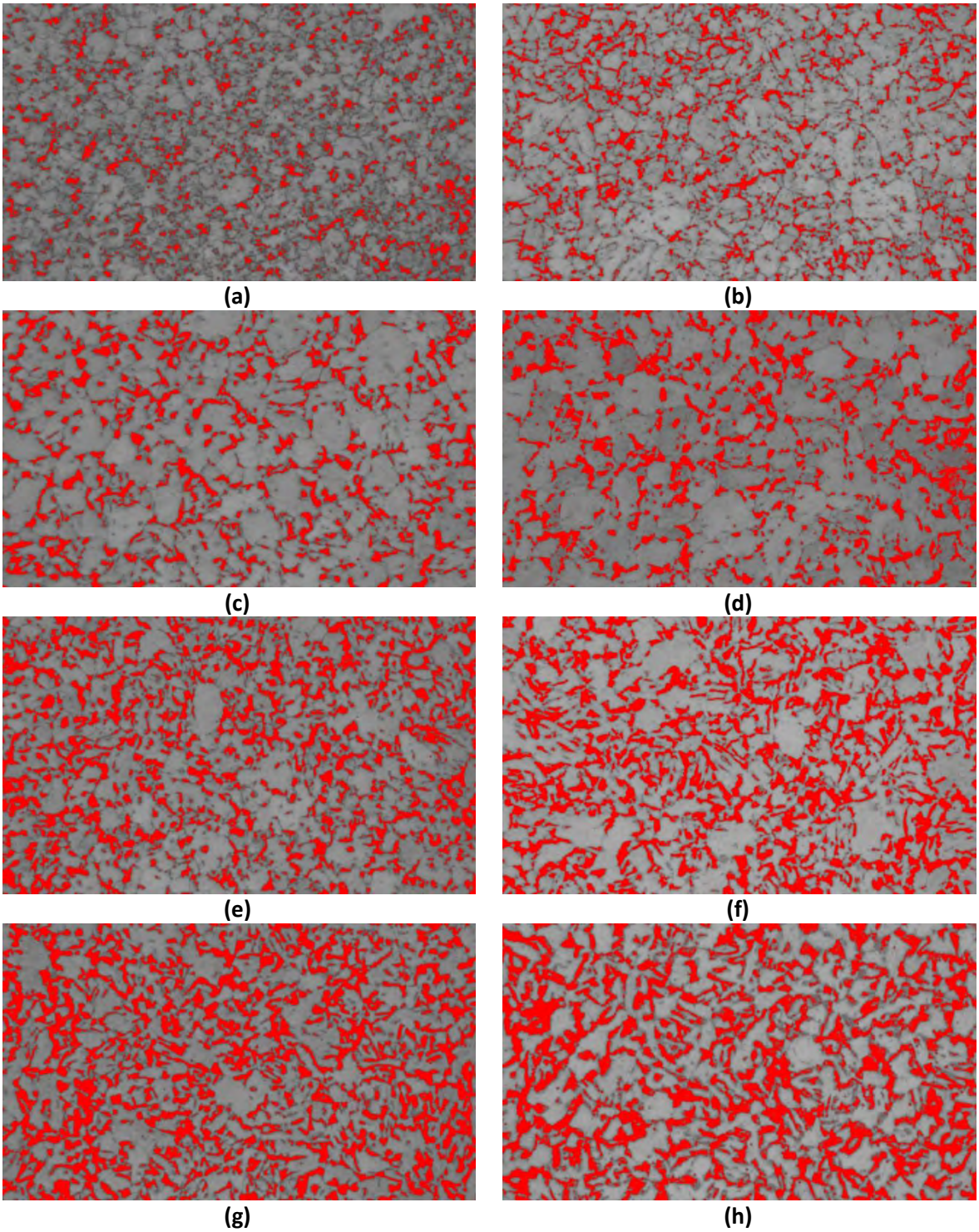

Figure 19: Intercritical annealing at 720°C for varying times 0.5 min (a), 1 min (b), 2 min (c), 3 min (d), 4 min (e) 5 min (f), 10 min (g) and 1 hour (h). Magnification of all images is x1000. The martensite volume fraction is noted in Table 8 below and is shown in all pictures in red.

Table 8: Volume fraction of martensite and ferrite with respect to IA holding time at 720°C.

Specimens (figure No)	Holding Time (min)	Volume Fraction Ferrite	Volume Fraction Martensite
a	**0.5**	92.49	7.51
b	**1**	87.80	12.2
c	**2**	85.46	14.54
d	**3**	81.89	18.11
e	**4**	76.86	23.14
f	**5**	72.83	27.17
g	**10**	71.17	28.83
h	**60**	70.77	29.23
Thermocalc		71.00	29

Image produced for image analysis for varying holding times at 750°C are presented in Figure 20. Magnification of all images is x1000 and holding time starts from 30sec up to 1 hour. In Figure 20 (a) the specimen subjected to IA heat treatment for 30sec is depicted. Light gray grains are observed, and they correspond to ferrite. Some very small areas in the triple points of the ferrite grain boundaries are observed denoted with red color. Figure 20 (b) depicts the specimen subjected to IA heat treatment for 60sec. For 60sec holding time a dispersion of small red areas is observed at the triple points of the ferrite grain boundaries. It is obvious that they are more easily distinguished than in the case of the 30sec holding time. As holding time progresses in Figure 20 (c) to 2min a similar microstructure is observed with light gray ferrite grain and red martensite grains. Martensite grains are larger than for 60sec IA holding time but still quite small and isolated by the larger ferrite grains. Holding time of 3min at 750°C in Figure 20 (d) produces even larger martensite grains growing intergranular to the ferrite grains. Larger holding time at 4min in Figure 20 (e) results in a more prominent change of the martensite phase as the smaller intergranular grains have grown and connected with each other, isolating larger ferrite grains. Holding time of 5min in Figure 20 (f) presents a similar behavior with connected larger martensite grains and isolated large ferrite grains. Figure 20 (g) and (h) depict micrographs for IA holding time 10 min and 1hour respectively, these micrographs exhibit similar behavior as in the case of 5min. The volume fraction of the respective phases are presented in Table 9. Volume fraction of martensite for 30sec IA is measured at 11.12% and it acquires higher values as IA holding time increases. For 1 hour holding time it is measured at 43.72% very close to the volume fraction of austenite calculated with Thermocalc.

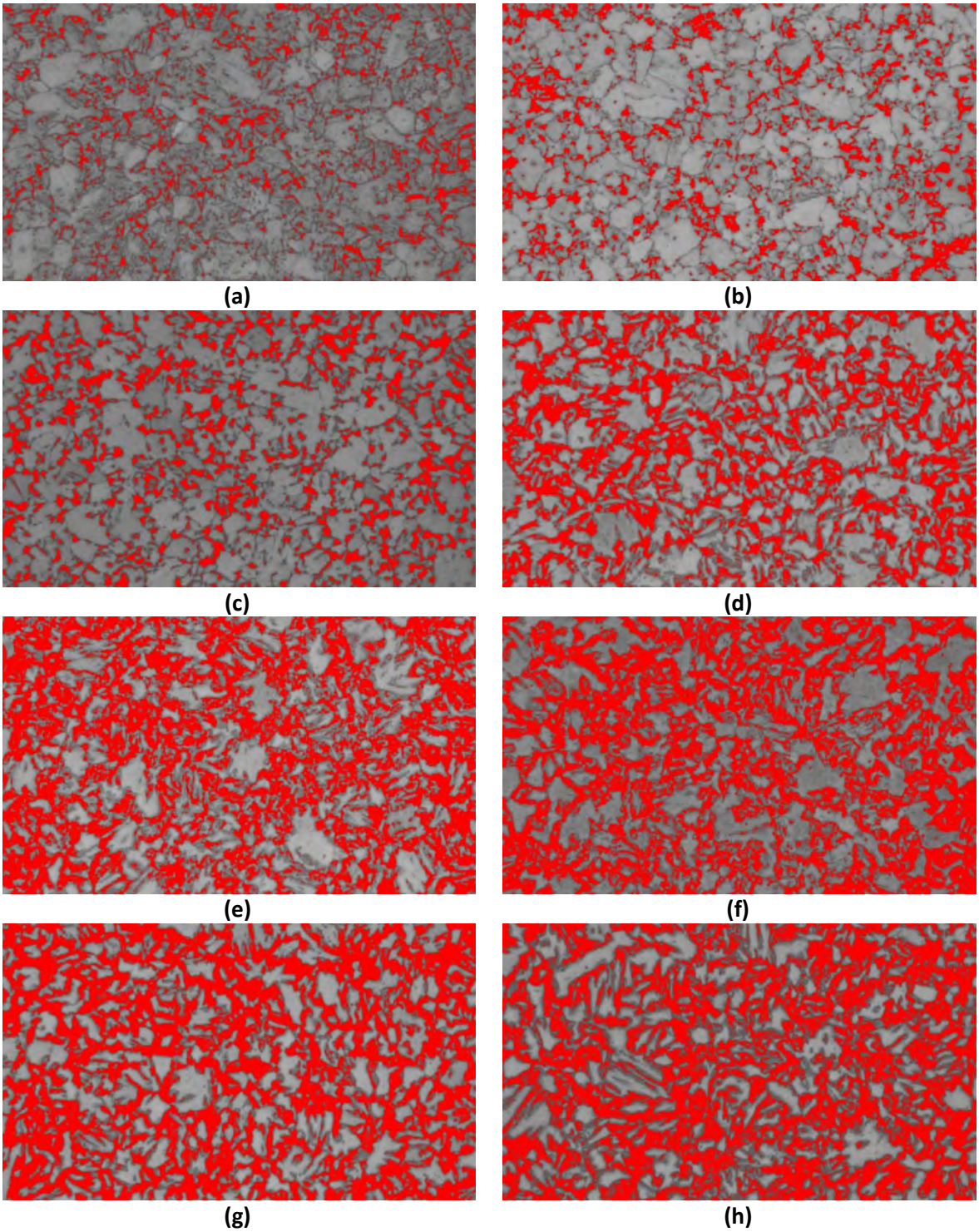

Figure 20: Intercritical annealing at 750°C for varying times 0.5 min (a), 1 min (b), 2 min (c), 3 min (d), 4 min (e) 5 min (f), 10 min (g) and 1 hour (h). Magnification of all images is x1000. The martensite volume fraction is noted in Table 8 below and is shown in all pictures in red.

Table 9: Volume fraction of martensite and ferrite with respect to IA holding time at 750°C.

Specimens (figure No)	Holding Time (min)	Volume Fraction Ferrite	Volume Fraction Martensite
a	**0.5**	88.88	11.12
b	**1**	81.95	18.05
c	**2**	76.78	23.22
d	**3**	69.77	30.23
e	**4**	62.52	37.48
f	**5**	60.68	39.32
g	**10**	57.18	42.82
h	**60**	56.28	43.72
Thermocalc		**56.20**	**43.80**

Image produced for image analysis for varying holding times at 760°C are presented in Figure 21. Magnification of all images is x1000 and holding time starts from 30sec up to 1 hour. In Figure 21 (a) the specimen subjected to IA heat treatment for 30sec is depicted. Light gray grains are observed, and they correspond to ferrite. Some very small areas in the triple points of the ferrite grain boundaries are observed denoted with red color. Figure 21 (b) depicts the specimen subjected to IA heat treatment for 60sec. For 60sec holding time a dispersion of small red areas is observed at the triple points of the ferrite grain boundaries. It is obvious that they are more easily distinguished than in the case of the 30sec holding time. These red areas represent martensite formed from prior austenite during quenching from the IA region. As holding time progresses in Figure 21 (c) to 2min a similar scenario is observed with light gray ferrite grain and red martensite grains. Martensite grains are larger than for 60sec IA holding time but still quite small and isolated by the larger ferrite grains. Holding time of 3min at 700°C in Figure 21 (d) produces even larger martensite grains growing intergranular to the ferrite grains. Larger holding time by only 1min at 4min in Figure 21 (e) results in a more prominent change of the martensite phase as the smaller intergranular grains have grown and connected with each other, isolating larger ferrite grains. Holding time of 5min in Figure 21 (f) presents a similar behavior with connected larger martensite grains and isolated large ferrite grains. Figure 21 (g) and (h) depict micrographs for IA holding time 10 min and 1hour respectively, these micrographs exhibit similar behavior as in the case of 5min. The volume fraction of the respective phases are presented in Table 10. Volume fraction of martensite for 30sec IA is measured at 13.38% and it acquires higher values as IA holding time increases. For 1 hour holding time it is measured at 50.07% equal to the volume fraction of austenite calculated with Thermocalc.

Image analysis results were not produced for the cases of intercritical annealing at higher temperatures 770 and 780°C, as the metallographic analysis could not produce sufficient contrast between the two phases.

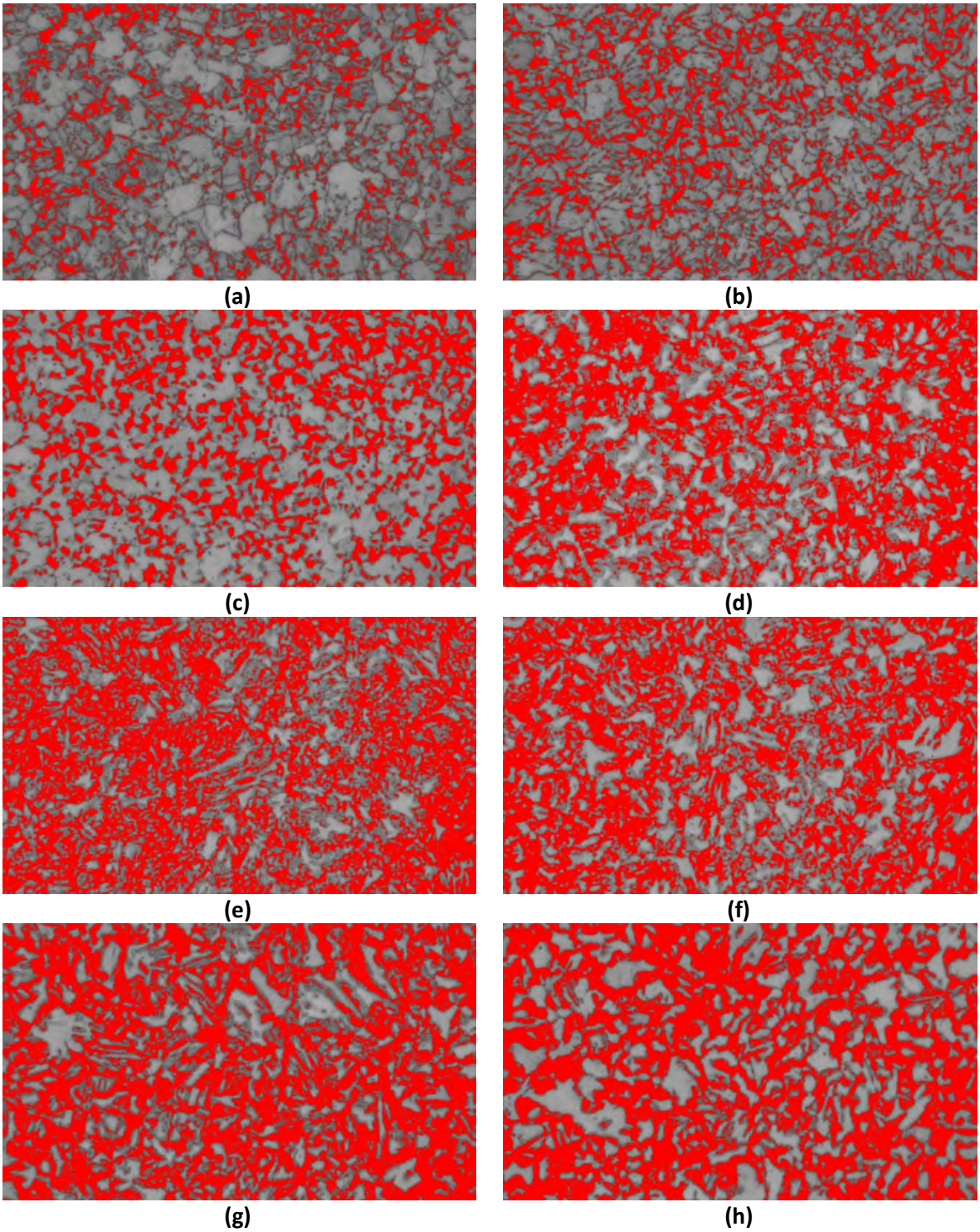

Figure 21: Intercritical annealing at 760°C for varying times 0.5 min (a), 1 min (b), 2 min (c), 3 min (d), 4 min (e) 5 min (f), 10 min (g) and 1 hour (h). Magnification of all images is x1000. The martensite volume fraction is noted in Table 8 below and is shown in all pictures in red.

Table 10: Volume fraction of martensite and ferrite with respect to IA holding time at 760°C.

Specimens (figure No)	Holding Time (min)	Volume Fraction Ferrite	Volume Fraction Martensite
a	**0.5**	86.62	13.38
b	**1**	77.96	22.04
c	**2**	69.04	30.96
d	**3**	59.77	40.23
e	**4**	54.38	45.62
f	**5**	50.50	49.50
g	**10**	50.03	49.97
h	**60**	49.93	50.07
Thermocalc		50.00	50.00

The volume fraction values measure during image analysis presented above were plotted with respect to interctitical annealing temperature and holding time and are presented in Figure 22. Time is in the logarithmic scale for better understanding of microstructural evolution at shorter times. Higher temperature produces more martensite and similarly larger IA holding times produce more at the same IA temperature.

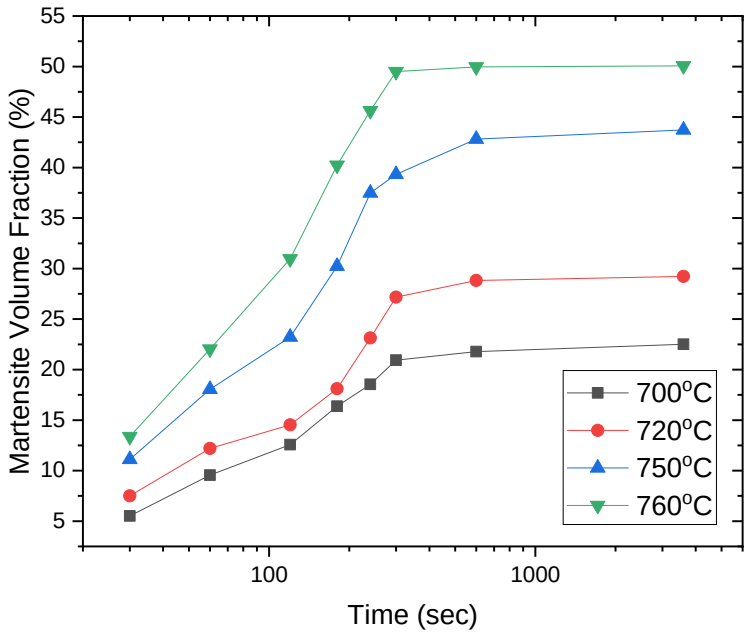

Figure 22: Volume fraction of transformed martensite after quenching from IA versus holding time (log scaling). Heat treatment temperatures are 700°C, 720°C, 750°C, 760°C.

3. Thermo Calc

Thermodynamic calculations of the proposed chemical composition mentioned in Table 1, with Thermo-Calc and TCFE6 database resulted in the phase diagram which is presented in Figure 23. The temperature at which austenite begins to form during heating (Ae_1) was calculated at 681.87°C and the temperature at which the transformation of ferrite to austenite is completed during heating (Ae_3) was calculated at 803.42°C.

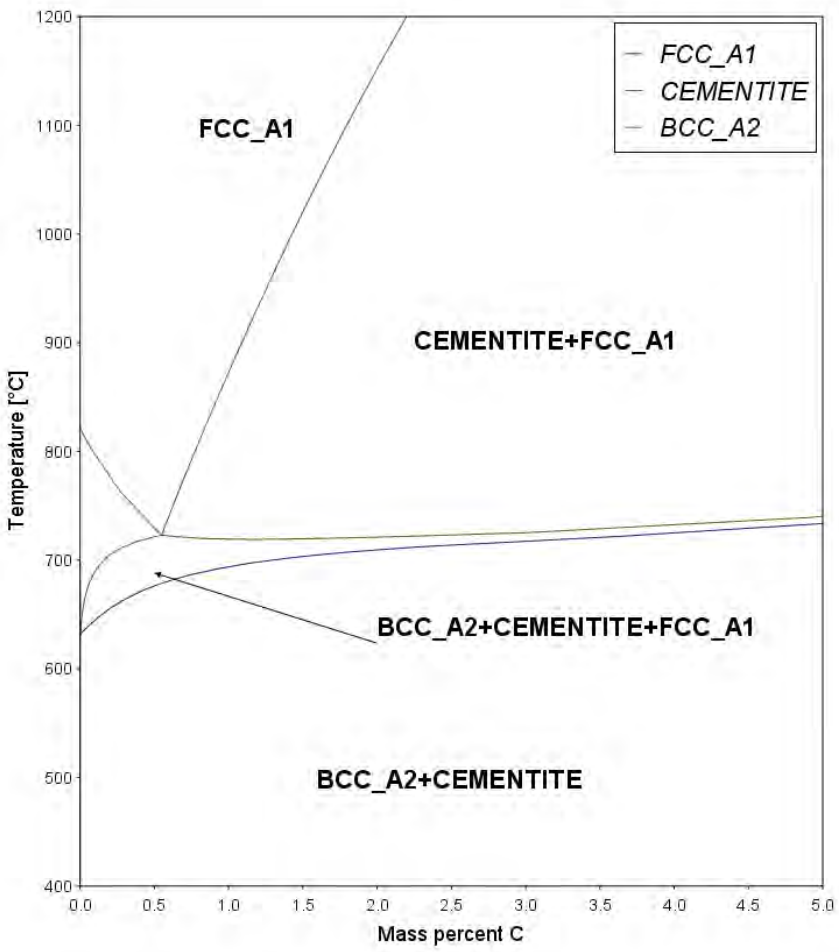

Figure 23: DP1000 Phase diagram. Calculated with THERMOCALC software and TCFE-6 database.

A magnification in the area of interest for the intercritical annealing heat treatment is depicted in Figure 24. The intecritical annealing two phase region, consisting of austenite and ferrite is denoted with an arrow as α+γ area. The isopleth diagram of DP1000 steel in Figure 24 is simplified. Ferrite is denoted as BCC_A2, austenite as FCC_A1 and cementite as CEMENTITE.

The collective data of mole fraction, mass fraction, activity and potential for all elements participating in DP1000 are presented in Table 11, as they were calculated with thermodynamics software Thermocalc.

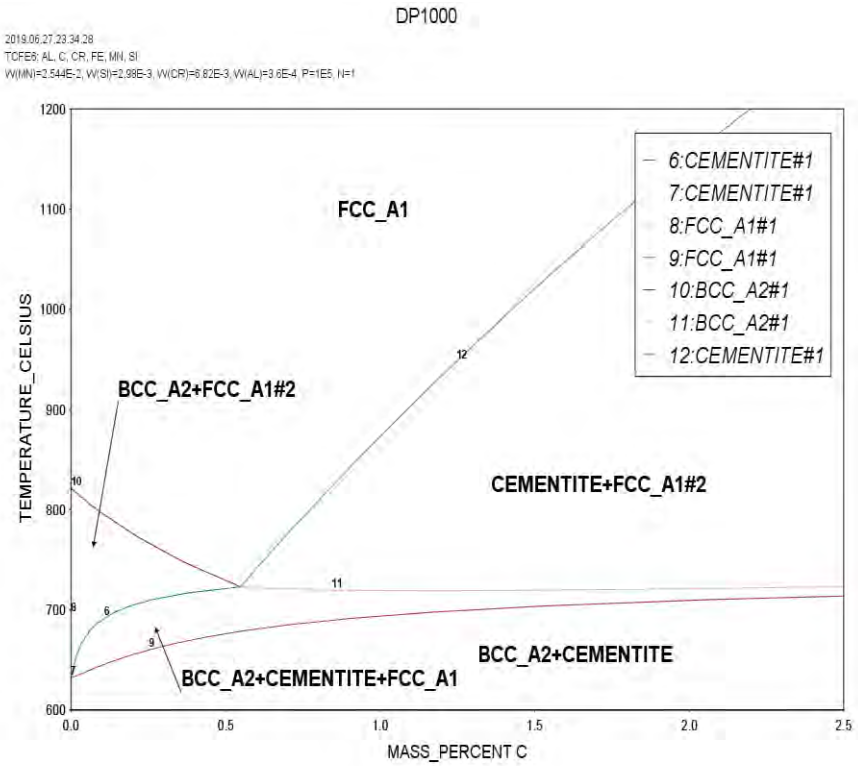

Figure 24: Simplified isopleth diagram of DP1000 steel. Calculated with THERMOCALC software and TCFE-6 database. Magnification of image in Figure 23.

Table 11: Collective data of mole fraction, mass fraction, activity and potential for all element participating in DP1000 calculate with Thermocalc.

Element	Mole Fraction	Mass Fraction	Activity	Potential
Cu	0,000952295	0,00109	0,000279	-69634,48
Fe	0,954102319	0,959758	0,005606	-44099,07
Ti	0,000833696	0,000719	4,82E-11	-202089,5
Si	0,005890599	0,00298	3,38E-10	-185509,4
C	0,003235578	0,0007	0,019975	-33290,38
Mn	0,025709545	0,025441	8,03E-05	-80220,08
Mo	0,000671261	0,00116	6,84E-05	-81585,85
W	4,83158E-05	0,00016	9,56E-06	-98327,38
V	7,30198E-05	6,7E-05	5E-08	-143008,7
Al	0,000740733	0,00036	2,22E-10	-189094,6
Cr	0,007281947	0,00682	0,000259	-70245,13
Co	4,23923E-05	4,5E-05	8,36E-08	-138636,6
Nb	0,000418299	0,0007	3,95E-10	-184193,5

Results regarding equilibrium intercritical annealing are presented in Table 12 to Table 17. In Table 12, results from ThermoCalc 2015a with TCFE6 database for thermodynamic equilibrium at 700^{o} C, are presented. The volume fraction of ferrite is 77.5%, while the remaining 22.5% is austenite, that after quenching it will resort in martensite.

Table 12: DP 1000 at thermodynamic equilibrium at 700° C, results from ThermoCalc 2015a with TCFE6 database.

Stable Phases	Moles	Mass	Volume Fraction
BCC_A2#1	0.77215	42.93739	0.700
FCC_A1#1	0.22785	12.53178	0.22446

In Table 13, results from ThermoCalc 2015a with TCFE6 database for thermodynamic equilibrium at 720° C, are presented. The volume fraction of ferrite is 70.9%, while the remaining 29.03% is austenite, that after quenching it will resort in martensite.

Table 13: DP 1000 at thermodynamic equilibrium at 720° C, results from ThermoCalc 2015a with TCFE6 database.

Stable Phases	Moles	Mass	Volume Fraction
BCC_A2#1	0.70584	39.24883	0.70961
FCC_A1#1	0.29416	16.22034	0.29039

In Table 14, results from ThermoCalc 2015a with TCFE6 database for thermodynamic equilibrium at 750° C, are presented. The volume fraction of ferrite is 56.1%, while the remaining 43.8% is austenite, that after quenching it will resort in martensite.

Table 14: DP 1000 at thermodynamic equilibrium at 750° C, results from ThermoCalc 2015a with TCFE6 database.

Stable Phases	Moles	Mass	Volume Fraction
BCC_A2#1	0.55772	31.01024	0.56187
FCC_A1#1	0.44228	24.45893	0.43813

In Table 15, results from ThermoCalc 2015a with TCFE6 database for thermodynamic equilibrium at 760° C, are presented. The volume fraction of ferrite is 49.1%, while the remaining 50.8% is austenite, that after quenching it will resort in martensite.

Table 15: DP 1000 at thermodynamic equilibrium at 760° C, results from ThermoCalc 2015a with TCFE6 database.

Stable Phases	Moles	Mass	Volume Fraction
BCC_A2#1	0.48707	27.08089	0.49117
FCC_A1#1	0.51293	28.38829	0.50883

In Table 16, results from ThermoCalc 2015a with TCFE6 database for thermodynamic equilibrium at 770° C, are presented. The volume fraction of ferrite is 40.6%, while the remaining 59.3% is austenite, that after quenching it will resort in martensite.

Table 16: DP 1000 at thermodynamic equilibrium at 770° C, results from ThermoCalc 2015a with TCFE6 database.

Stable Phases	Moles	Mass	Volume Fraction
BCC_A2#1	0.40294	22.40159	0.40679
FCC_A1#1	0.59706	33.06758	0.59321

In Table 17, results from ThermoCalc 2015a with TCFE6 database for thermodynamic equilibrium at 780° C, are presented. The volume fraction of ferrite is 30.6%, while the remaining 69.3% is austenite, that after quenching it will resort in martensite.

Table 17: DP 1000 at thermodynamic equilibrium at 780° C, results from ThermoCalc 2015a with TCFE6 database.

Stable Phases	Moles	Mass	Volume Fraction
BCC_A2#1	0.30322	16.85655	0.30653
FCC_A1#1	0.69678	38.61263	0.69347

The major result from these calculations is the fact that with increasing the intrecritical annealing temperature the volume fraction of austenite increases as well (Figure 25).

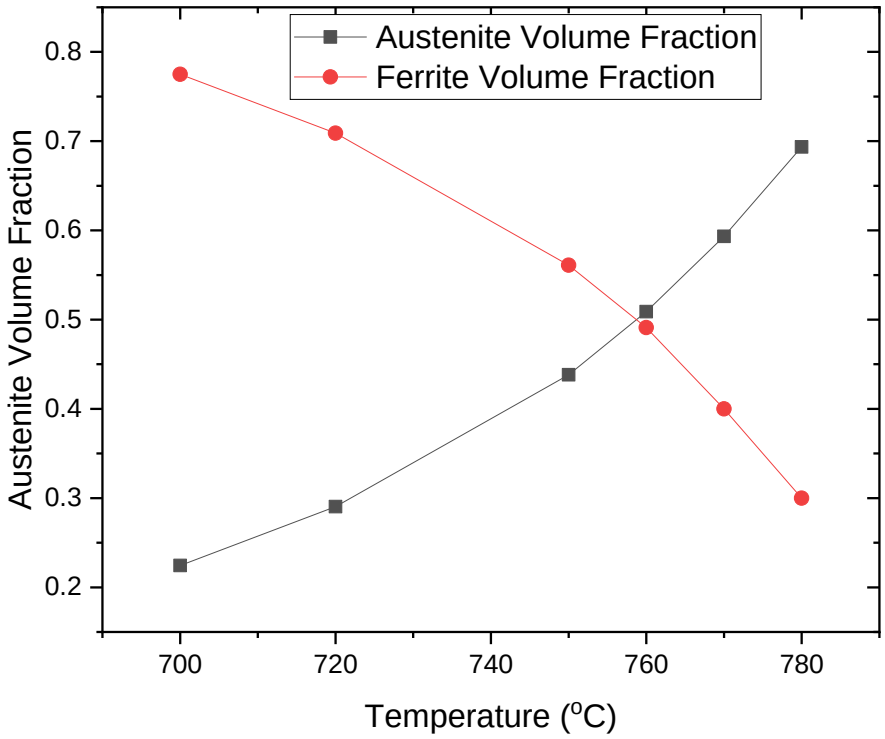

Figure 25: Austenite (f_γ) and ferrite (f_α) volume fraction versus intercritical annealing temperatures calculated with ThermoCalc 2015a (TCFE6 database). Results from Table 12 to Table 17.

4. Micro hardness

Microhardness measurements were performed for all specimens. Figure 26 depicts the microhardness measurements of specimens heated in the intercritical annealing region at 700°C versus holding time. For times up to 3 min of IA the microhardness increases, with peak microhardess at 3min at 290HV. After 3min the microhardness drops continuously until 10 min IA time (266HV) and peaks up again at 1 h (284HV). The microhardness values remain quite low.

Figure 27 depicts the microhardness measurements of specimens heated in the intercritical annealing region at 720°C versus holding time. The behavior of the material for 720°C is different than 700°C for short times, as the microhardness values initially drop to 256HV, but peak up after 3min and thereafter display a similar behavior with the specimen subjected to 700°C IA temperature. Overall the specimens at 720°C display higher microhardness values than that at 700°C, at the highest value reaching 313HV .

Figure 28 depicts the microhardness measurements of specimens heated in the intercritical annealing region at 750°C versus holding time. The material when subjected at 750°C display different behavior than for lower IA temperatures. A plateau is reached around 350HV for all holding times up to 10 min and at 1 h there a small drop in microhardness values. The overall microhardness values are higher than at 720°C.

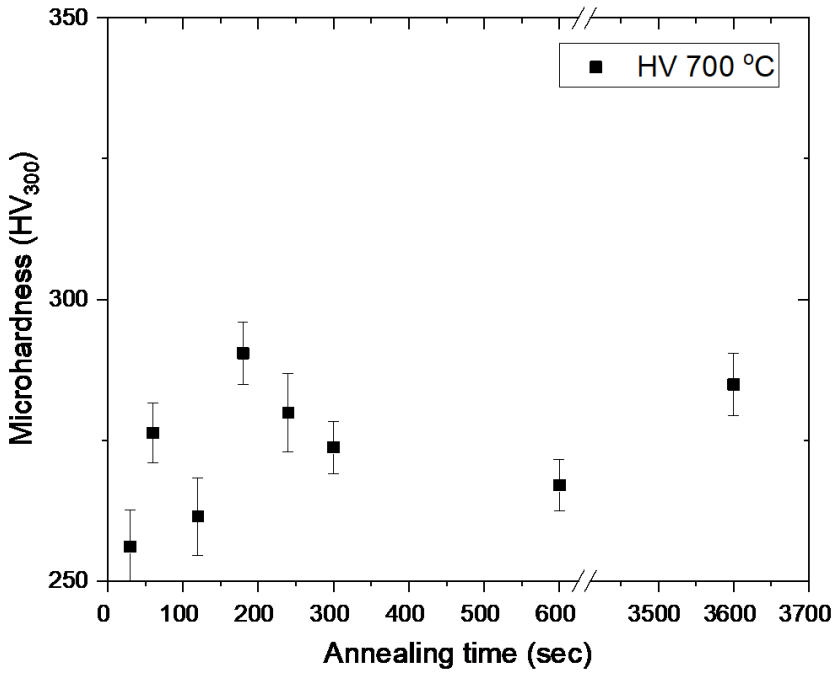

Figure 26: Microhardness measurements for specimens after quenching from IA at 700°C versus holding time.

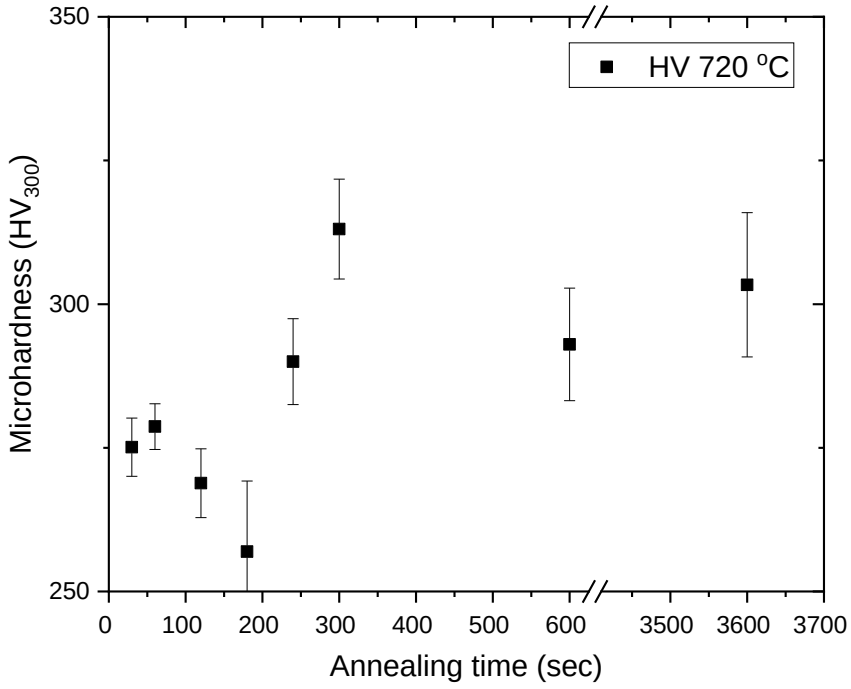

Figure 27: Microhardness measurements for specimens after quenching from IA at 720°C versus holding time.

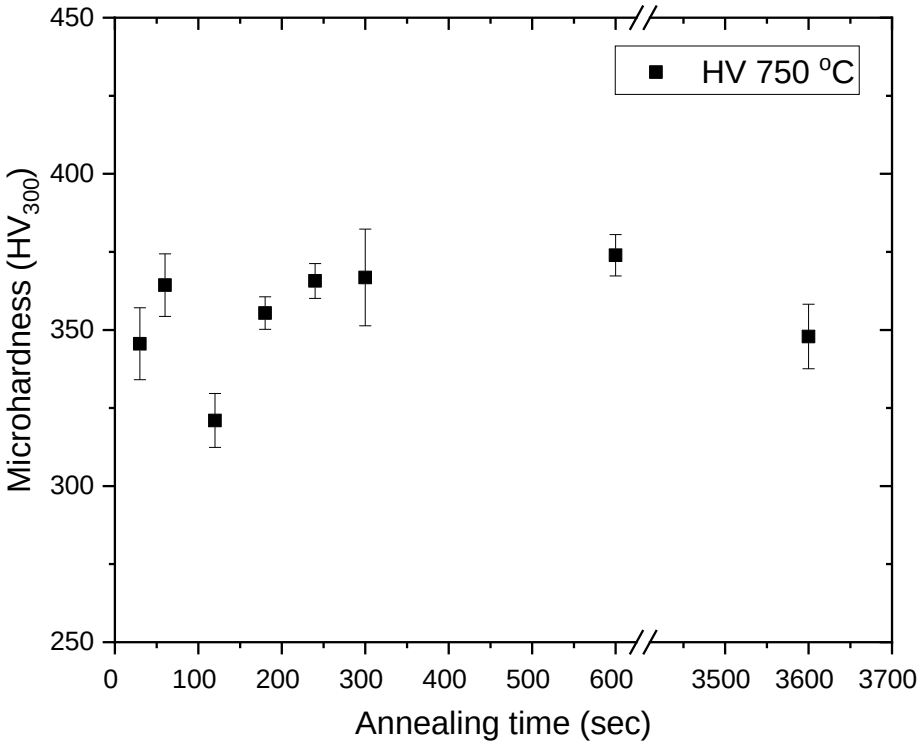

Figure 28: Microhardness measurements for specimens after quenching from IA at 750°C versus holding time.

Figure 29 depicts the microhardness measurements of specimens heated in the intercritical annealing region at 760°C versus holding time. Microharness starts at around 300HV for short annealing times increases to 400HV for 3min, maintains a plateau at 400HV up to 10min IA time and then drops at 1h to 350HV. The initial rise is attributed to the rise in martensite volume fraction while the final drop in microhardness values to the depletion of carbon from austenite. The overall microhardnes s values are higher than at 750°C. This drop can be explained by the IA at 770°C produces similar results as depicted in Figure 30. Intercritical annealing at 780°C produces similar results as 760°C and 770°C but the plateau of high values is considerably smaller (only 1min) as depicted in Figure 31.

Figure 32 to Figure 35 illustrate the microhardness profiles of specimen subjected to IA at 700°C, 720°C, 750°C and 760°C compared to the respective martensite volume fraction (f_{MART}), as it was calculated during image analysis of the corresponding micrographs.

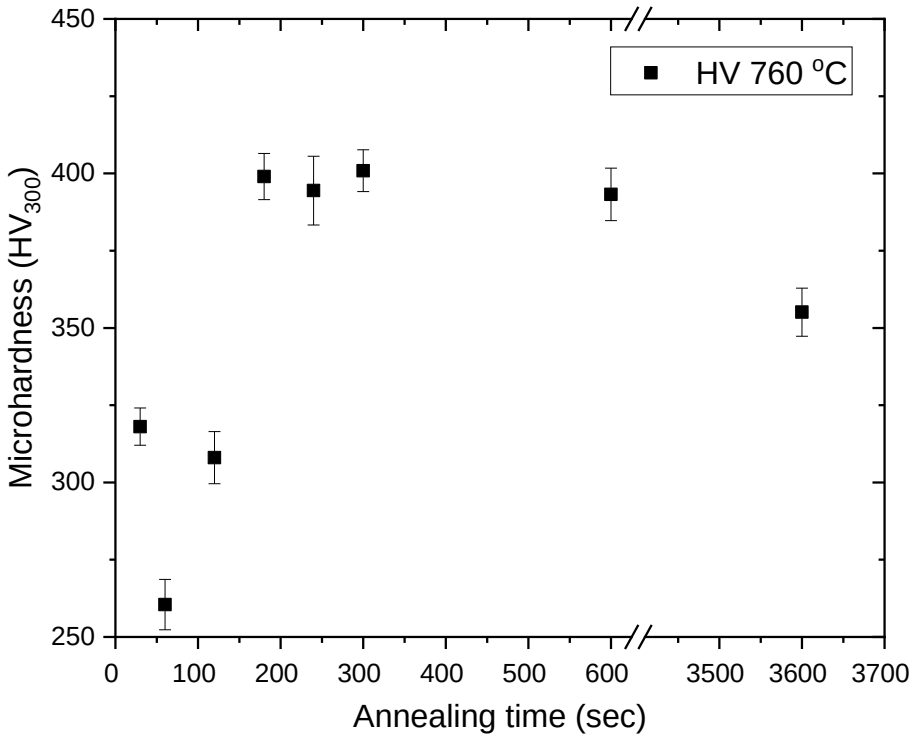

Figure 29: Microhardness measurements for specimens after quenching from IA at 760°C versus holding time.

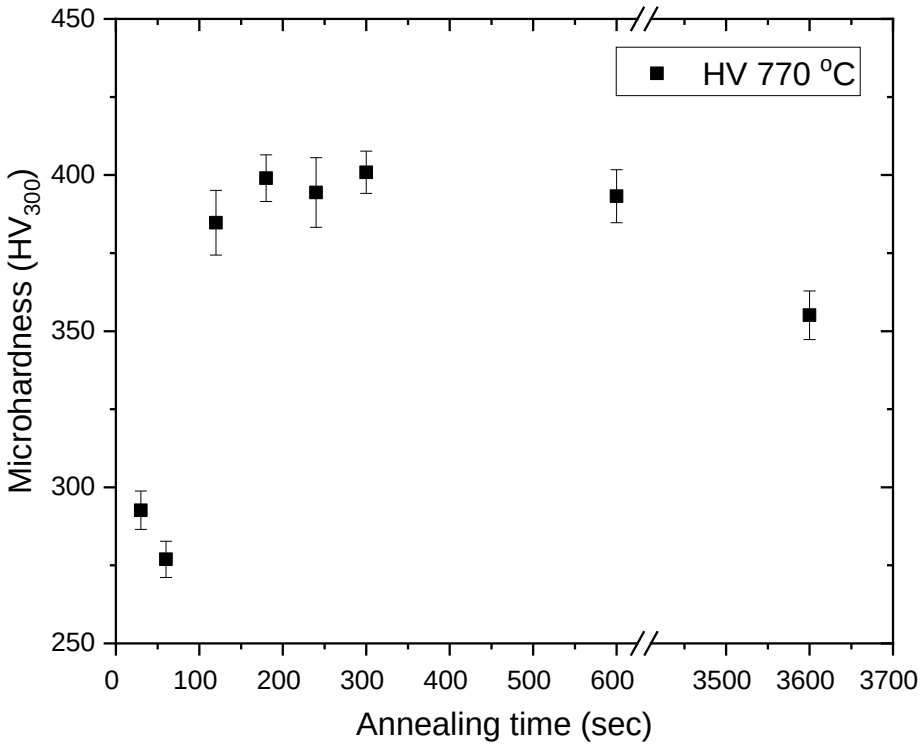

Figure 30: Microhardness measurements for specimens after quenching from IA at 770°C versus holding time.

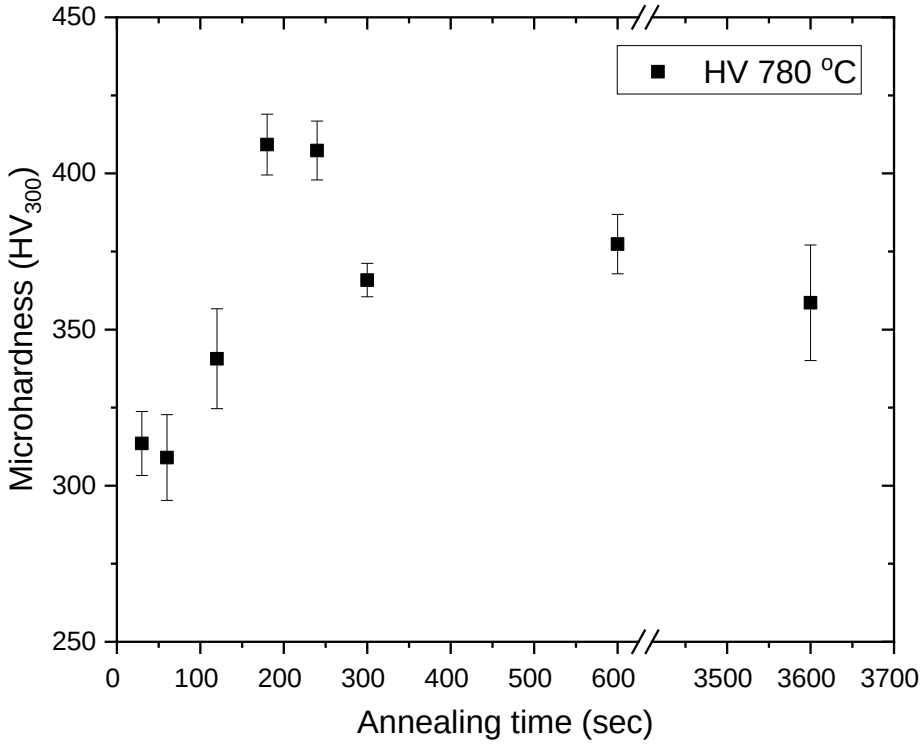

Figure 31: Microhardness measurements for specimens after quenching from IA at 780°C versus holding time.

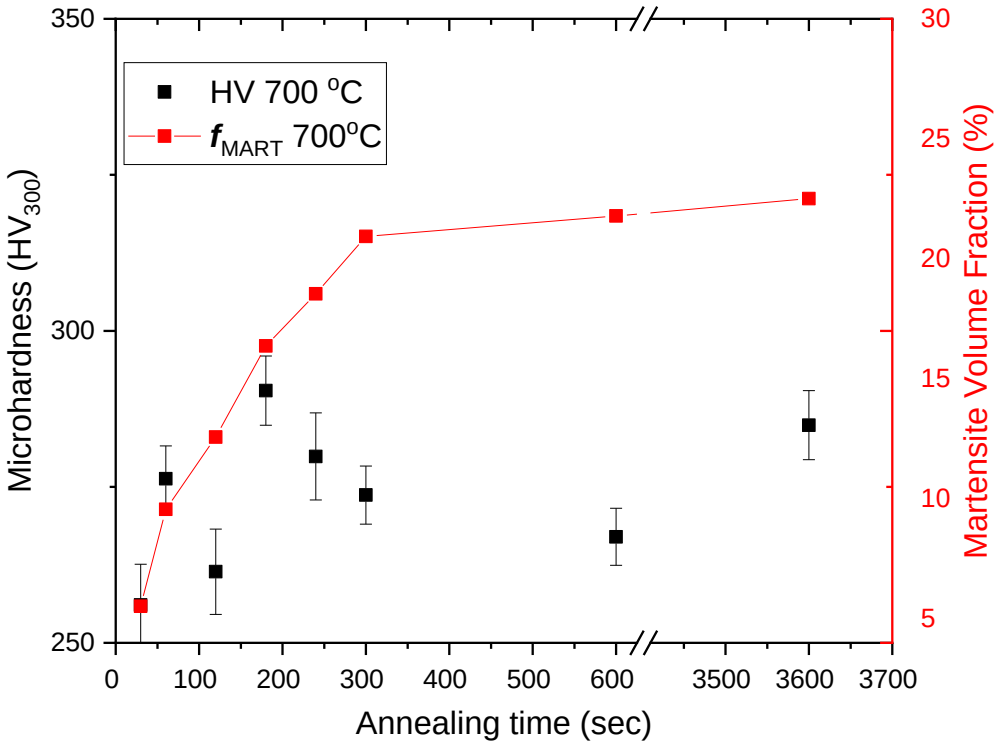

Figure 32: Microhardness measurements for specimens after quenching from IA at 700°C versus holding time comparison with the volume fraction of transformed martensite (f_{MART}) after quenching from IA versus holding time. Heat treatment temperature is 700°C.

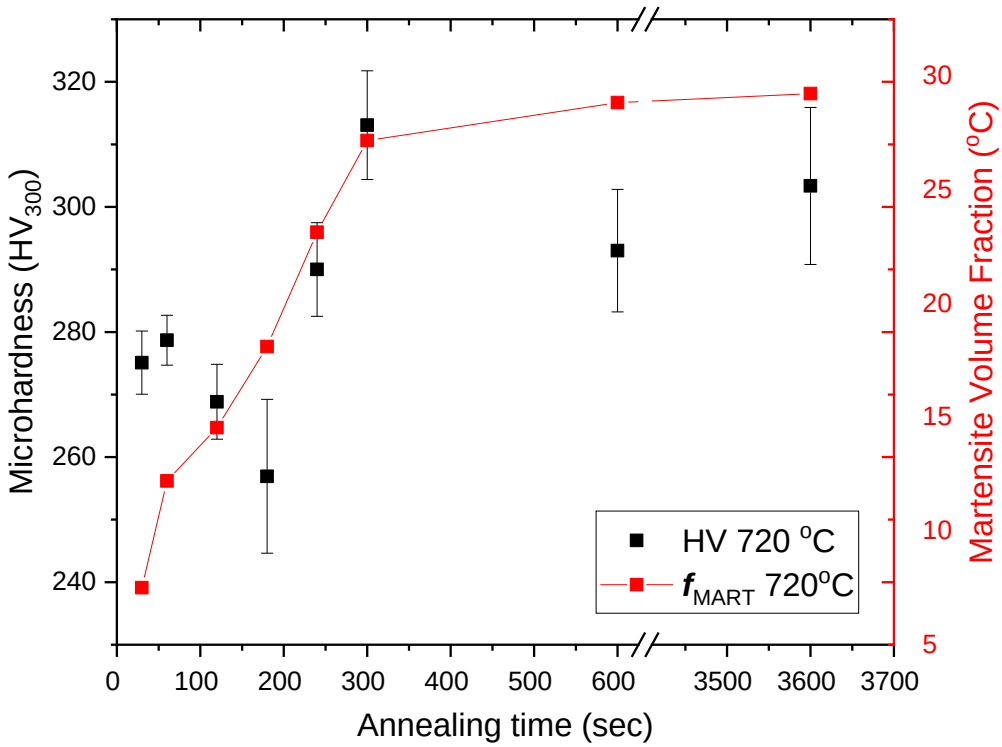

Figure 33: Microhardness measurements for specimens after quenching from IA at 720°C versus holding time comparison with the volume fraction of transformed martensite (f_{MART}) after quenching from IA versus holding time. Heat treatment temperature is 720°C.

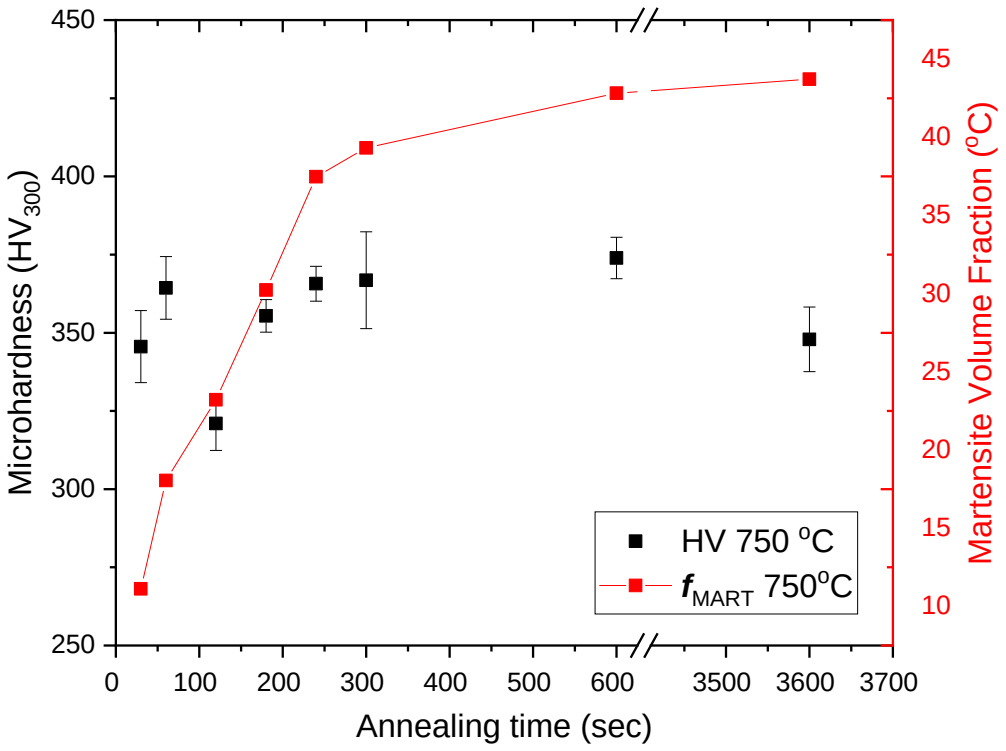

Figure 34: Microhardness measurements for specimens after quenching from IA at 750°C versus holding time comparison with the volume fraction of transformed martensite (f_{MART}) after quenching from IA versus holding time. Heat treatment temperature is 750°C.

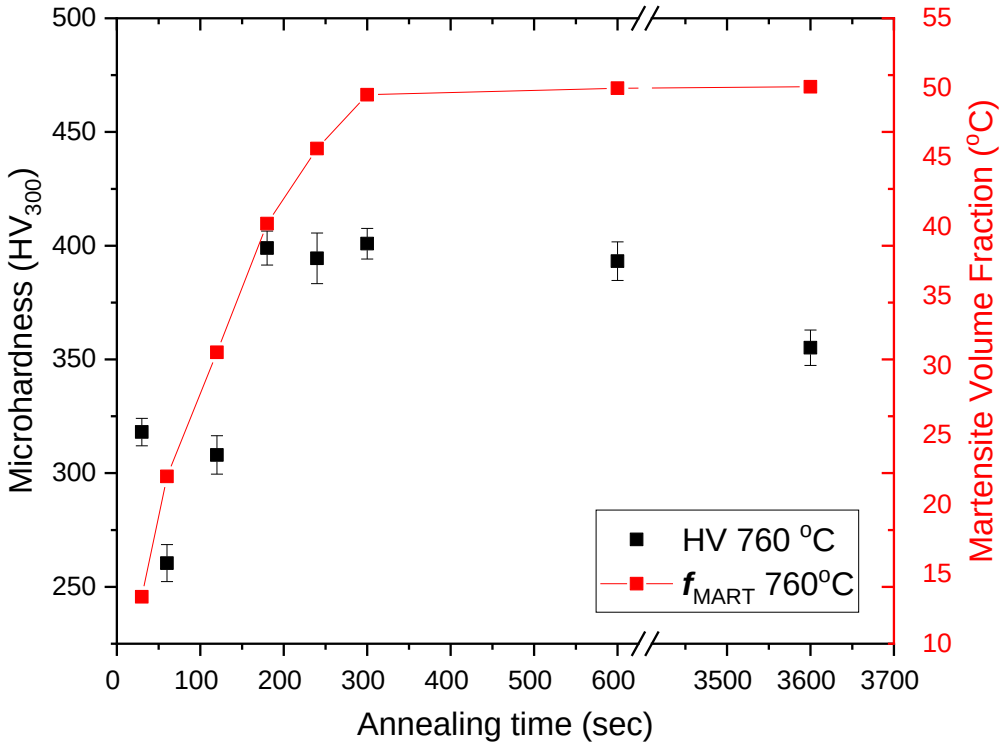

Figure 35: Microhardness measurements for specimens after quenching from IA at 760°C versus holding time comparison with the volume fraction of transformed martensite (f_{MART}) after quenching from IA versus holding time. Heat treatment temperature is 760°C.

Chapter 5: Concluding Discussion

For high holding times in the intercritical annealing range, it seems that in all occasions, specimens reach the thermodynamic equilibrium and the anticipated martensite volume fraction as it results from the Thermo Calc software. Image J software contributed to that calculation of martensite as it counted blackened regions of each specimen, which correspond according to the two stage Nital-Metabisulfite technique to martensitic regions. However, an image analysis method like this is possible to lead to false conclusions as dark regions can be confused with grain boundaries or pearlite or retained austenite regions. For that reason there is an error in this method. To restrict or preferentially totally eliminate this error, it is advisable to use a deeper investigation such as a SEM (Scanning Electron Microscopy) method.

Returning to the image analysis method, it can be certainly said that for low annealing temperatures in the intercritical spectrum, evolution of austenite becomes much slower than for higher IA temperatures. That means that for low temperatures, higher times are demanded to reach the thermodynamic equilibrium. On the other hand, for higher annealing temperatures, this equilibrium is reached for much lower times. Moreover, from Thermo Calc software, it can be pointed that for high annealing temperatures, higher martensite volume fractions can be obtained. The average grain size of ferrite varies, while martensite can exhibit two different shapes. Equiaxed and plate like martensite.

Microhardness measurements were performed. For the two lower temperatures 700^{o}C and 720^{o}C after a microhardness peak at about 3min microhardness drops continuously until 10 min IA time and then peaks up again at 1 h. The microhardness values remain quite low. In the case of 750^{o}C the material displays different behavior than for lower IA temperatures. A plateau is reached around 350HV for all holding times up to 10 min and at 1 h there a small drop in microhardness values. The overall microhardness values are higher than at 720^{o}C. Higher IA temperatures 760^{o}C and 770^{o}C produce gradual rise in the microhardness, a subsequent a plateau at about 400HV up to 10min IA and a final drop after 1h to around 350HV. The initial rise is attributed to the rise in martensite volume fraction while the final drop in microhardness values to the depletion of carbon from austenite. The overall microhardnes s values are higher than at 750^{o}C. This drop can be explained by the maintains. For the highest temperature 780^{o}C the plateau is very small.

For the desired DP 1000 50-50 percentage, it seems that 760^{o} C would be ideal as it reaches 50.8% austenite at equilibrium situation. Another good candidate temperature is 760^{o}C as reaches 50% austenite at much sorter times and exhibits higher microdardness values (400HV). These two heat treatments seem good candidates for an equal amount of the two dominant phases to be obtained combined with the optimum mechanical properties.

Chapter 6: Future Work

DP steels, and more specifically DP 1000 steel is a material with a wide use mainly in automotive industry. For that reason, in recent years, more and more researches are carried out with a main and ultimate goal; the optimization of mechanical properties via microstructure control. Such a technique for microstructure study and control is presented in the present work.

Nevertheless, there are many more research topics concerning this type of steel. One of them is the study of the kinetics of austenite formation at higher temperatures by dilatometry. From the length changed of the heat-treated specimens, the percentage of austenite formed at various times and temperatures can be calculated.

Another study concerning DP steels is investigating via Atomic Force Microscopy (AFM) of the microhardness of individual phases (martensite and ferrite). Microhardness can be performed tests in a very small region of the material. In the present study, micro hardness tests became with a load of the order of 300 grams leaving a trace, whose area is equal to a couple of grains. An in-grain micro hardness test with loads of the order of 10 grams could be performed. The contribution of each phase to the aggregate micro hardness value could be evaluated.

Chapter 7: References

1. Terada, D., et al., *Reason for high strength and good ductility in dual phase steels composed of soft ferrite and hard martensite.* IOP Conference Series: Materials Science and Engineering, 2017. **219**: p. 012008.
2. Bergström, Y., Y. Granbom, and D. Sterkenburg, *A Dislocation-Based Theory for the Deformation Hardening Behavior of DP Steels: Impact of Martensite Content and Ferrite Grain Size %J Journal of Metallurgy.* 2010. **2010**: p. 16.
3. *Steel DP-W and PD-K Product information for dual-phase steels*, thyssenkrupp, Editor. 2018.
4. Haidemenopoulos, G., *Physical Metallurgy*. 2007, Greece: Tziolas. 736.
5. Tasan, C.C., et al., *An Overview of Dual-Phase Steels: Advances in Microstructure-Oriented Processing and Micromechanically Guided Design.* Annual Review of Materials Research, 2015. **45**(1): p. 391-431.
6. Papa Rao, M., et al., *Microstructure and Mechanical Properties of V-Nb Microalloyed Ultrafine-Grained Dual-Phase Steels Processed Through Severe Cold Rolling and Intercritical Annealing.* 2017. **48**(3): p. 1176-1188.
7. Matsumura, N. and M. Tokizane, *Microstructure and the Mechanical Properties of Dual-phase Steel Produced by Intercritical Annealing of Lath Martensite.* Tetsu-to-Hagane, 1984. **70**(2): p. 246-253.
8. Honeycombe, R.W.K. and H.K.D.H. Bhadeshia, *Steels : microstructure and properties*. 2nd ed. Metallurgy and materials science series. 1996, London, New York: Arnold ; Halsted Press.
9. Speich, G.R., V.A. Demarest, and R.L. Miller, *Formation of Austenite During Intercritical Annealing of Dual-Phase Steels.* Metallurgical and Materials Transactions A, 1981. **12**(8): p. 1419-1428.
10. Huang, J., W.J. Poole, and M. Militzer, *Austenite formation during intercritical annealing.* Metallurgical and Materials Transactions a-Physical Metallurgy and Materials Science, 2004. **35a**(11): p. 3363-3375.
11. Azizi-Alizamini, H., M. Militzer, and W.J. Poole, *Austenite Formation in Plain Low-Carbon Steels.* Metallurgical and Materials Transactions A, 2010. **42**(6): p. 1544-1557.
12. Brands, D., et al., *Computational modeling of dual-phase steels based on representative three-dimensional microstructures obtained from EBSD data.* Archive of Applied Mechanics, 2016. **86**(3): p. 575-598.
13. Rudnizki, J., et al., *Phase-Field Modeling of Austenite Formation from a Ferrite plus Pearlite Microstructure during Annealing of Cold-Rolled Dual-Phase Steel.* Metallurgical and Materials Transactions A, 2011. **42**(8): p. 2516-2525.
14. Peranio, N., F. Roters, and D. Raabe, *Microstructure Evolution during Recrystallization in Dual-Phase Steels.* Materials Science Forum, 2012. **715-716**: p. 13-22.
15. Peranio, N., et al., *Microstructure and texture evolution in dual-phase steels: Competition between recovery, recrystallization, and phase transformation.* Materials Science and Engineering: A, 2010. **527**(16): p. 4161-4168.
16. Ogawa, T., *Ferrite recrystallization and austenite formation at the early stage of annealing in cold-rolled low-carbon steels.* International Journal of Mechanical and Materials Engineering, 2015. **10**(1): p. 22.
17. Lanzillotto, C. and F. B. Pickering, *Structure–property relationships in dual-phase steels*. Vol. 16. 1982. 371-382.
18. Zheng, C. and D. Raabe, *Interaction between recrystallization and phase transformation during intercritical annealing in a cold-rolled dual-phase steel: A cellular automaton model.* Acta Materialia, 2013. **61**(14): p. 5504-5517.
19. Huang, J., W.J. Poole, and M. Militzer, *Austenite formation during intercritical annealing.* Metallurgical and Materials Transactions A, 2004. **35**(11): p. 3363-3375.
20. Andrews, K.W., *Empirical Formulae for the Calculation of Some transformation Temperatures.* JISI, 1965. **203**: p. 721–727.

21. Movahed, P., et al., *The effect of intercritical heat treatment temperature on the tensile properties and work hardening behavior of ferrite–martensite dual phase steel sheets.* Materials Science and Engineering: A, 2009. **518**(1): p. 1-6.
22. Speich, G.R., V.A. Demarest, and R.L. Miller, *Formation of Austenite during Intercritical Annealing of Dual-Phase Steels.* Metallurgical Transactions a-Physical Metallurgy and Materials Science, 1981. **12**(8): p. 1419-1428.
23. Peng-Heng, C. and A.G. Preban, *The effect of ferrite grain size and martensite volume fraction on the tensile properties of dual phase steel.* Acta Metallurgica, 1985. **33**(5): p. 897-903.
24. Jiang, Z., Z. Guan, and J. Lian, *Effects of microstructural variables on the deformation behaviour of dual-phase steel.* Materials Science and Engineering: A, 1995. **190**(1): p. 55-64.
25. Toolkit for the design of damage tolerant microstructures, *Research Programme of the Research Fund for Coal and Steel, Grant Agreement Number: 709711,.* 2016.
26. Suwanpinij, P., *Multi-scale Modelling of Hot Rolled Dual-phase Steels for Process Design*. 2012, RWTH: Aachen.
27. Bocharova, E., et al., *Dual-phase steel, flat product made of such dual-phase steel and method for manufacturing a flat product* E.P. Office, Editor. 2007: Germany.
28. Voort, G.F.v.d., *Metallography*. 1984, New York, Hamburg: McGraw-Hill.